



# **UNDERSTANDING HOST FACTORS IN *DANIO RERIO* THAT REGULATE ALPHAVIRUS INFECTION**

Submitted By:  
Sethu Ananthakrishnan Sanjith (S10225028A)

Final Year Project Report  
Diploma in Biomedical Science  
April 2025 – August 2025

Supervisor: Dr Guillaume Carissimo  
Co-Supervisor: Dr Claire Honney  
Co-Supervisor (NP): Dr New Jen Yan

**School of Life Sciences and Chemical Technology**

**Ngee Ann Polytechnic**

## I. Declaration

I declare that this report titled "Understanding host factors in *Danio rerio* that regulate alphavirus infection", submitted to the School of Life Sciences & Chemical Technology, is my original work. Any information or materials from other sources have been referenced and acknowledged accordingly.

Name: Sethu Ananthakrishnan Sanjith

Signature: Sanjith

Date: 26 July 2025

## II. Abstract

Alphaviruses, such as Chikungunya virus (CHIKV), pose a significant global health risk; however, the pathogen-host factor interactions responsible for controlling infection remain poorly understood. *Danio rerio* (zebrafish) are a good disease model because they are genetically similar to humans and are optically transparent. In this project, zebrafish were used to investigate the differential viral tropism of genetically modified alphaviruses and the role of MXRA8A, an alphavirus receptor, and IRF3, a key regulator of the immune pathway, on alphavirus infection. Crispants of MXRA8A and IRF3 were generated through the injection of CRISPR/Cas9 with guide RNAs (gRNA) at the single-cell stage of zebrafish development. Two days after CRISPR/Cas9 injection, zebrafish embryos were infected with alphaviruses, mainly CHIKV and Virus X (unnamed due to confidentiality), and their structural protein swaps. MXRA8A crispants led to an increased infection of Virus X, suggesting an unexpected antiviral role for MXRA8A. IRF3 depletion led to an increased infection of CHIKV, indicating an expected antiviral role, as it is a key innate immune regulator. Additionally, wild-type (WT) AB strain zebrafish were infected with CHIKV and a chimeric variant of CHIKV (CHIKV XnsP4), containing the RNA-dependent RNA polymerase (RdRp) of Virus X. CHIKV XnsP4 consistently showed a higher proportion of zebrafish exhibiting localization of the virus to the swim bladder of zebrafish during infection. The RdRp is not part of the structural components of the virus, so its ability to influence viral tropism opens a novel role for non-structural proteins in influencing infection. These findings highlight the ability of zebrafish as a powerful *in vivo* model for studying host factor-virus interactions to reveal previously unknown or unseen phenotypes for further study.

### III. Acknowledgement

As I conclude this project, I would like to express my sincere gratitude towards my supervisor, Dr. Guillaume Carissimo, as well as my co-supervisor, Dr. Claire Honney, for giving me this tremendous opportunity to learn under their professional guidance and supervision. I would also like to thank Dr. Samuel Tong and Dr. New Jen Yan for providing me with endless help and support. I greatly appreciate Dr. Guillaume for giving me the chance to work in the Host-pathogens Interaction laboratory at Infectious Diseases Labs, Agency for Science, Technology and Research (A\*STAR). I would also like to give thanks to Mr. Lim Ming Xuan, Ms. Estelle Goh, and Mr. Ng Hong Xiang for their kind assistance during this period. This project is funded by the National Medical Research Council, Open Fund Investigator Research Grant (MOH-OFIRG24jan-0012).

## IV. Table of contents

I. DECLARATION .....	II
II. ABSTRACT .....	III
III. ACKNOWLEDGEMENT .....	IV
IV. TABLE OF CONTENTS .....	V
V. LIST OF FIGURES AND TABLES .....	VII
LIST OF FIGURES .....	VII
LIST OF TABLES .....	VIII
VI. LIST OF ABBREVIATIONS .....	IX
1. INTRODUCTION .....	1
1.1 OVERVIEW OF ALPHAVIRUSES.....	1
1.1.1 <i>Epidemiology and impact of alphaviruses</i> .....	1
1.1.2 <i>Chikungunya virus</i> .....	2
1.1.3 <i>Impact in Singapore</i> .....	4
1.2 GENOME ORGANIZATION OF ALPHAVIRUSES AND VIRAL REPLICATION .....	5
1.3 ALPHAVIRUS ENTRY AND CURRENTLY KNOWN HOST FACTOR INTERACTIONS .....	9
1.3.1 <i>Versatility of alphavirus entry</i> .....	9
1.3.2 <i>MXRA8</i> .....	9
1.3.3 <i>IRF3</i> .....	10
1.3.4 <i>Other receptors</i> .....	11
1.4 <i>DANIO RERIO</i> AS A TRANSLATIONAL MODEL .....	12
1.4.1 <i>Danio rerio is an ideal whole-vertebrate model</i> .....	12
1.4.2 <i>Disadvantages of using Danio rerio as an animal model</i> .....	13
1.4.3 <i>Rapid genetic modification of Danio rerio</i> .....	13
1.5 KNOWLEDGE GAP AND STUDY RATIONALE .....	15
1.6 PROJECT OBJECTIVES .....	16
2. METHODS AND MATERIALS .....	17
2.1 ZEBRAFISH MAINTENANCE AND PREPARATION .....	17
2.2 EVALUATING THE DIFFERENCE IN ALPHAVIRUS INFECTION BETWEEN CRISPANT ZEBRAFISH.....	18
2.2.1 <i>Knockout zebrafish generation via CRISPR/Cas9 technology</i> .....	18

2.2.2 Virus strains and fluorescent reporters.....	20
2.2.3 Infection of zebrafish larvae.....	20
2.2.4 Fluorescence imaging of infected zebrafish.....	21
2.2.5 High Resolution Melt (HRM) analysis.....	22
2.3 DETERMINE IF PROTEIN D OF VIRUS X RESULTS IN SWIM BLADDER LOCALIZATION OF ALPHAVIRUSES.....	23
2.3.1 Infecting zebrafish with alphaviruses.....	24
2.3.2 Fluorescence imaging of infected zebrafish.....	24
2.3.3 Cryosectioning and immunofluorescence.....	25
<b>3. RESULTS.....</b>	<b>26</b>
3.1 SWIM BLADDER LOCALIZATION CAUSED BY CHIKV XnsP4 COMPARED TO CHIKV WT.....	26
3.1.1 Optimizing zebrafish injection techniques .....	32
3.1.2 Optimizing CHIKV XnsP4 infection .....	36
3.1.3 Consolidation of swim bladder localization results .....	39
3.2 GENETIC DEPLETION OF MXRA8A AND IRF3 AFFECTS ALPHAVIRUS INFECTION IN ZEBRAFISH .....	40
3.2.1 Effect of MXRA8A in alphavirus infection in zebrafish.....	41
3.2.2 Effect of IRF3 in alphavirus infection in zebrafish.....	43
3.2.3 High Resolution Melt analysis of crispant zebrafish.....	47
<b>4. DISCUSSION .....</b>	<b>49</b>
4.1 TROPISM OF CHIMERIC CHIKV XnsP4 VIRUS.....	49
4.2 MXRA8A AND IRF3 CRISPANTS ZEBRAFISH AFFECT THE INFECTIVITY OF CERTAIN ALPHAVIRUSES IN ZEBRAFISH .....	53
<b>5. CONCLUSION AND FUTURE WORK.....</b>	<b>59</b>
<b>6. REFERENCES.....</b>	<b>62</b>

## V. List of Figures and Tables

### List of Figures

<b>FIGURE 1.</b> SCHEMATIC DIAGRAM OF THE ALPHAVIRUS GENOME. DIAGRAM TAKEN FROM PATHOGENICITY AND VIRULENCE OF O'NYONG-NYONG VIRUS: A LESS STUDIED TOGAVIRIDAE WITH PANDEMIC POTENTIAL BY TONG ET AL., 2024.....	5
<b>FIGURE 2.</b> DIAGRAM DESCRIBING THE REPLICATION CYCLE OF ONNV, AN OLD-WORLD ALPHAVIRUS THAT IS HIGHLY SIMILAR TO CHIKV. DIAGRAM TAKEN FROM PATHOGENICITY AND VIRULENCE OF O'NYONG-NYONG VIRUS: A LESS STUDIED TOGAVIRIDAE WITH PANDEMIC POTENTIAL BY TONG ET AL., 2024.....	7
<b>FIGURE 3.</b> A SCHEMATIC DIAGRAM THAT OVERVIEWS THE EXPERIMENTAL PLAN TO EVALUATE WHETHER THE PRESENCE OR ABSENCE OF SPECIFIC GENES CAUSES UPREGULATION OR DOWNREGULATION OF ALPHAVIRUS INFECTION.....	18
<b>FIGURE 4.</b> A SCHEMATIC DIAGRAM THAT OVERVIEWS THE ENTIRE EXPERIMENTAL PLAN TO EVALUATE IF THE RdRp OF VIRUS X RESULTS IN SWIM BLADDER LOCALIZATION OF ALPHAVIRUSES.....	23
<b>FIGURE 5.</b> QUANTIFICATION OF CHIKV WT AND CHIKV XnsP4 INFECTION IN WILD-TYPE AB ZEBRAFISH BASED ON THE INTENSITY OF ZsGREEN FLUORESCENCE.....	27
<b>FIGURE 6.</b> IMAGES OF TRANSVERSE SECTIONS OF ZEBRAFISH INFECTED WITH CHIKV WT. (A) IS THE BRIGHTFIELD IMAGE OF A SECTION OF ZEBRAFISH INFECTED WITH CHIKV WT AT 10X MAGNIFICATION. (B) IS THE BRIGHTFIELD IMAGE OF A SECTION OF ZEBRAFISH INFECTED WITH CHIKV WT AT 60X MAGNIFICATION. (C) IS THE GFP IMAGE OF A SECTION OF ZEBRAFISH INFECTED WITH CHIKV WT AT 60X MAGNIFICATION. (D) IS THE MERGED IMAGE OF BOTH BRIGHTFIELD AND GFP IMAGES.....	29
<b>FIGURE 7.</b> IMAGES OF TRANSVERSE SECTIONS OF ZEBRAFISH INFECTED WITH CHIKV XnsP4. (A) IS THE BRIGHTFIELD IMAGE OF A SECTION OF ZEBRAFISH INFECTED WITH CHIKV XnsP4 AT 10X MAGNIFICATION. (B) IS THE BRIGHTFIELD IMAGE OF A SECTION OF ZEBRAFISH INFECTED WITH CHIKV XnsP4 AT 60X MAGNIFICATION. (C) IS THE GFP IMAGE OF A SECTION OF ZEBRAFISH INFECTED WITH CHIKV XnsP4 AT 60X MAGNIFICATION. (D) IS THE MERGED IMAGE OF BOTH BRIGHTFIELD AND GFP IMAGES.....	30
<b>FIGURE 8.</b> COMPARISON OF THE PROPORTION OF SWIM BLADDER LOCALIZATION OF VIRUS OBSERVED BETWEEN CHIKV WT AND CHIKV XnsP4 IN EXPERIMENT 1.....	31
<b>FIGURE 9.</b> QUANTIFICATION OF CHIKV WT AND CHIKV XnsP4 INFECTION (EXPERIMENT 2) IN WILD-TYPE AB ZEBRAFISH BASED ON THE INTENSITY OF ZsGREEN FLUORESCENCE .....	33
<b>FIGURE 10.</b> COMPARISON OF THE PROPORTION OF SWIM BLADDER LOCALIZATION OF VIRUS OBSERVED BETWEEN CHIKV WT AND CHIKV XnsP4 IN EXPERIMENT 2.....	35
<b>FIGURE 11.</b> QUANTIFICATION OF CHIKV WT AND CHIKV XnsP4 INFECTION (EXPERIMENT 3) IN WILD-TYPE AB ZEBRAFISH BASED ON THE INTENSITY OF ZsGREEN FLUORESCENCE .....	37

<b>FIGURE 12.</b> COMPARISON OF THE PROPORTION OF SWIM BLADDER LOCALIZATION OF VIRUSES OBSERVED BETWEEN CHIKV WT AND CHIKV XnSP4 IN EXPERIMENT 3.....	38
<b>FIGURE 13.</b> COMPARISON OF THE PROPORTION OF SWIM BLADDER LOCALIZATION OF VIRUS OBSERVED BETWEEN CHIKV WT AND CHIKV XnSP4 ACROSS EXPERIMENTS 1 & 3. ....	39
<b>FIGURE 14.</b> QUANTIFICATION OF ALPHAVIRUS INFECTION IN MXRA8A CRISPANTS COMPARED TO SCRAM CONTROL ZEBRAFISH BASED ON THE INTENSITY OF ZSGREEN FLUORESCENCE .....	41
<b>FIGURE 15.</b> QUANTIFICATION OF ALPHAVIRUS INFECTION IN IRF3 CRISPANTS COMPARED TO SCRAM CONTROL ZEBRAFISH (REPLICATE 1) BASED ON THE INTENSITY OF ZSGREEN FLUORESCENCE .....	43
<b>FIGURE 16.</b> QUANTIFICATION OF ALPHAVIRUS INFECTION IN IRF3 CRISPANTS COMPARED TO SCRAM CONTROL ZEBRAFISH (REPLICATE 2) BASED ON THE INTENSITY OF ZSGREEN FLUORESCENCE. ....	45
<b>FIGURE 17.</b> DIFFERENCE AND MELT CURVES GENERATED AFTER HRM ANALYSIS. (A) IS THE DIFFERENCE CURVE GENERATED FROM MXRA8A CRISPANTS, SCRAM ZEBRAFISH (POSITIVE CONTROL), AND NTC. (B) IS THE MELT CURVE GENERATED FROM MXRA8A CRISPANTS, SCRAM ZEBRAFISH (POSITIVE CONTROL), AND NTC. (C) IS THE DIFFERENCE CURVE GENERATED FROM IRF3 CRISPANTS, SCRAM ZEBRAFISH (POSITIVE CONTROL), AND NTC. (D) IS THE MELT CURVE GENERATED FROM IRF3 CRISPANTS, SCRAM ZEBRAFISH (POSITIVE CONTROL), AND NTC. ....	47

## List of Tables

<b>TABLE 1.</b> gRNA SEQUENCES USED FOR CRISPR/Cas9 .....	19
<b>TABLE 2.</b> PRIMERS USED FOR HRM ANALYSIS .....	22

## VI. List of abbreviations

Abbreviation	Full form
BSA	Bovine Serum Albumin
CHIKV	Chikungunya virus
CHIKV XnsP4	Chikungunya virus with the RNA-dependent RNA polymerase of Virus X and ZsG reporter
CHIKV WT	Wild-Type Chikungunya virus with ZsG reporter
CHIKV XSP	Chikungunya virus with the Structural Proteins of Virus X and ZsG reporter
X CSP	Virus X with Chikungunya virus Structural Proteins and ZsG reporter
CRISPR	Clustered regularly interspaced short palindromic repeats
DAPI	4',6-Diamidino-2-Phenylindole
DC-SIGN	Dendritic Cell-Specific Intercellular Adhesion Molecule-3-Grabbing Non-Integrin
dpf	Days post-fertilization
dpi	Days post-infection
ECSA	East/Central/South African Lineage
EEEV	Eastern equine encephalitis virus
gDNA	Genomic DNA
HRM	High Resolution Melt
IFN	Interferon

IRF3	Interferon Regulatory Factor 3
LDLR	Low-density lipoprotein receptor
MXRA8(A)	Matrix Remodeling Associated Protein 8(a)
nsP	Non-structural protein
OCT	Optimal Cutting Temperature compound
ONNV	O'nyong'nyong virus
ORF	Open Reading Frame
PAM	Protospacer Adjacent Motif
PCR	Polymerase chain reaction
PTU	Phenylthiourea
qPCR / RT-qPCR	Quantitative PCR / Reverse-transcription quantitative PCR
RRV	Ross river virus
RdRp	RNA-dependent RNA polymerase
SINV	Sindbis virus
VEEV	Venezuelan equine encephalitis virus
WEEV	Western equine encephalitis virus
WT	Wild-type
ZsG	Zoanthus-derived green fluorescent protein

# 1. Introduction

## 1.1 Overview of alphaviruses

### 1.1.1 Epidemiology and impact of alphaviruses

Alphaviruses are positive-sense RNA viruses belonging to the *Togaviridae* family and are primarily vector-borne, transmitted via mosquitoes (Lantz and Baxter, 2025; Ma *et al.*, 2020). They are either grouped based on their clinical syndromes or their geographical location. Chikungunya virus (CHIKV), Ross river virus (RRV), Sindbis Virus (SINV), and O'nyong-nyong virus (ONNV) are arthritogenic, causing joint swelling and inflammation (Ma *et al.*, 2020). On the other hand, Eastern (EEEV), Western (WEEV), and Venezuelan (VEEV) equine encephalitic viruses are encephalitic, causing swelling of the brain (Ma *et al.*, 2020). Alphaviruses can also be categorized based on their geographical location as “New World” or “Old World” and typically correlate with the symptoms of disease (arthritogenic or encephalitic) induced in humans (Lantz and Baxter, 2025). Old World viruses, typically found in Africa, Europe, Asia, and Australia, cause systemic diseases characterized by symptoms such as headache, fever, and malaise, as well as arthritic and arthralgic conditions (Paredes *et al.*, 2006; Lantz and Baxter, 2025). CHIKV, ONNV, and RRV are examples of Old World viruses (Lantz and Baxter, 2025). In contrast, New World viruses such as EEEV, WEEV, and VEEV are generally found in the Americas and typically lead to neurological disease and pathology (Paredes *et al.*, 2006; Lantz and Baxter, 2025). Many endemics and large epidemics have been caused by these viruses

throughout Africa, Asia, and the Americas in the past century, making them an important group of viruses to study (Azar *et al.*, 2020; Suhrbier, Jaffar-Bandjee and Gasque, 2012).

### 1.1.2 Chikungunya virus

Among the alphaviruses, Chikungunya virus (CHIKV) has been of interest due to its capacity for rapid spread, resulting in millions of infections, and often causes a fever accompanied by severe arthralgia (Hoornweg *et al.*, 2016). A total of 480,000 cases and over 200 deaths were reported globally in 2024 alone (*Chikungunya virus disease worldwide overview*, 2025). An outbreak in 2004 in Kenya led to the largest CHIKV epidemic of more than 6 million cases, with the virus spreading to India and parts of Southeast Asia (Silva and Dermody, 2017). In 2005, CHIKV emerged in the Indian Ocean islands: Comoros, Mayotte, Seychelles, Réunion, and Mauritius, causing one of the most significant outbreaks of CHIKV, and in 2006, an estimated 244,000 cases were reported out of a total population of 770,000 in Réunion (Schuffenecker *et al.*, 2006). The viral strain responsible for this outbreak belongs to the East, Central, South African (ECSA) genotype (Frumence *et al.*, 2025). In 2023, another major CHIKV epidemic occurred in Minas Gerais, a highly populated state in Brazil, resulting in over 890 deaths (Freitas *et al.*, 2024). In 2024, the Indian National Centre for Vector Borne Diseases Control reported more than 231,000 suspected cases, with more than 17,800 confirmed cases of CHIKV (Hiscox *et al.*, 2025). India continues to have a significant number of CHIKV cases to this day.

Currently, three phylogenetic lineages of CHIKV have been identified: ECSA, West African, and Asian (De Lima Cavalcanti *et al.*, 2022). As of the beginning of June 2025, more than 33,000 CHIKV cases have been reported in Asia (*Chikungunya virus disease worldwide overview*, 2025).

It is known that different alphaviruses use different and often specific species of mosquitoes as their vector. Vector specificity is dependent on the interactions between the viral surface proteins and specific receptors found in the mosquitoes, which facilitate successful infection and transmission. (Lantz and Baxter, 2025). The primary vector for CHIKV is the mosquito *Aedes aegypti*, although a mutation in the viral E1 glycoprotein (A226V) identified during the ECSA-lineage outbreak in 2004 led to *Aedes albopictus* becoming a vector as well, contributing to CHIKV's increased capacity to spread globally (Desdouits *et al.*, 2015; Weaver *et al.*, 2012).

Although CHIKV infection is usually self-limiting, some patients develop persistent long-term joint pain that lasts for months or years, affecting their quality of life across physical, cognitive, psycho-emotional, and sociocultural domains (Santos *et al.*, 2024; Weaver *et al.*, 2012). Despite being widely researched, CHIKV currently has no approved antiviral treatments or licensed vaccines to protect against the disease (Weaver *et al.*, 2012).

### 1.1.3 Impact in Singapore

Singapore experienced a significant outbreak of CHIKV in 2008 with 718 laboratory-confirmed cases (Jupp *et al.*, 2008). This outbreak was caused by a CHIKV strain related to the ECSA genotype that emerged in the Indian Ocean region in 2005 (Ng *et al.*, 2009). A second outbreak in Singapore occurred in 2013, resulting in 1,059 confirmed cases despite intensive vector control (*Communicable Diseases Surveillance in Singapore*, 2013). A serological study later conducted in 2021 using sera collected from 2009, 2013, and 2017 revealed that less than 2% of Singapore residents have CHIKV-neutralizing antibodies, meaning that the lack of available antivirals or vaccines for CHIKV leaves 98% of Singaporeans immunologically naïve and would be prone to CHIKV infection (Hapuarachchi *et al.*, 2021).

Controlling the population of mosquitoes to prevent mosquito-borne viruses such as CHIKV incurs a significant financial burden (Chee *et al.*, 2016). In 2013, the National Environmental Agency (NEA) allocated S\$85 million for research, elimination of mosquito breeding, and public education (See, 2013). In addition, Singapore's ageing population leads to the government allocating a larger proportion of the budget to be invested in the healthcare sector to support older people, which limits the budget for other sectors.

## 1.2 Genome organization of alphaviruses and viral replication

Studying the structure and replication process of alphaviruses is crucial for understanding host-pathogen interactions and the mechanisms of viral replication. Alphaviruses are enveloped viruses with a single-stranded, capped, positive-sense RNA genome approximately 11.8kb in size (Zimmerman *et al.*, 2023). The genome has a 5' methyl-guanosine cap and a 3' polyadenine tail (Solignat *et al.*, 2009).

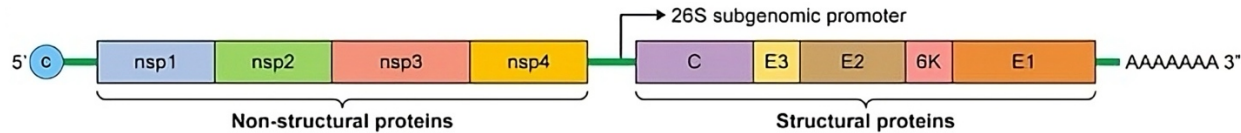


**Figure 1.** Schematic diagram of the Alphavirus genome. Diagram taken from *Pathogenicity and virulence of O'nyong-nyong virus: A less studied Togaviridae with pandemic potential* by Tong *et al.*, 2024.

As seen in **Figure 1**, the alphavirus genome is divided into two open-reading frames (ORFs) (Zimmerman *et al.*, 2023). The first ORF is located in the 5' two-thirds of the genome, which encodes for the non-structural proteins (nsPs) of the virus that are essential for the viral replication machinery (**Figure 1**). The second ORF encodes for structural proteins (SPs) consisting of either viral capsid protein (CP), envelope proteins (E) of E3, E2, 6K, and E1, or by ribosomal frameshift as a CP-E3-E2 TransFrame protein (TF) (**Figure 1**, Tong *et al.*, 2024; Shin *et al.*, 2012). E1 and E2 are transmembrane glycoproteins, which interact to form heterodimers that further assemble into 80 trimeric spikes on the alphavirus surface (Holmes *et al.*, 2020). The host immune system typically

recognizes these spikes to suppress virus infection. E2 is also responsible for host cell receptor binding, while E1 mediates membrane fusion after endocytosis (Holmes *et al.*, 2020). The C-terminal domain of E2 engages with the capsid protein to stabilize the virion (Holmes *et al.*, 2020). E3 is a small glycoprotein that plays a role in the translocation of p62, the precursor of E2, into the Endoplasmic Reticulum (ER) and also plays a role in the transport of both E2 and E1 to the plasma membrane (Uchime, Fields and Kielian, 2013). The 6K protein facilitates glycoprotein maturation and spike assembly (Uchime, Fields and Kielian, 2013). TF is present at lower levels on the virion surface and is associated with E1/E2 complexes (Holmes *et al.*, 2020). Palmitoylation of TF has been shown to suppress type I interferon response, although the exact mechanism of this is yet to be understood (Rogers *et al.*, 2020).

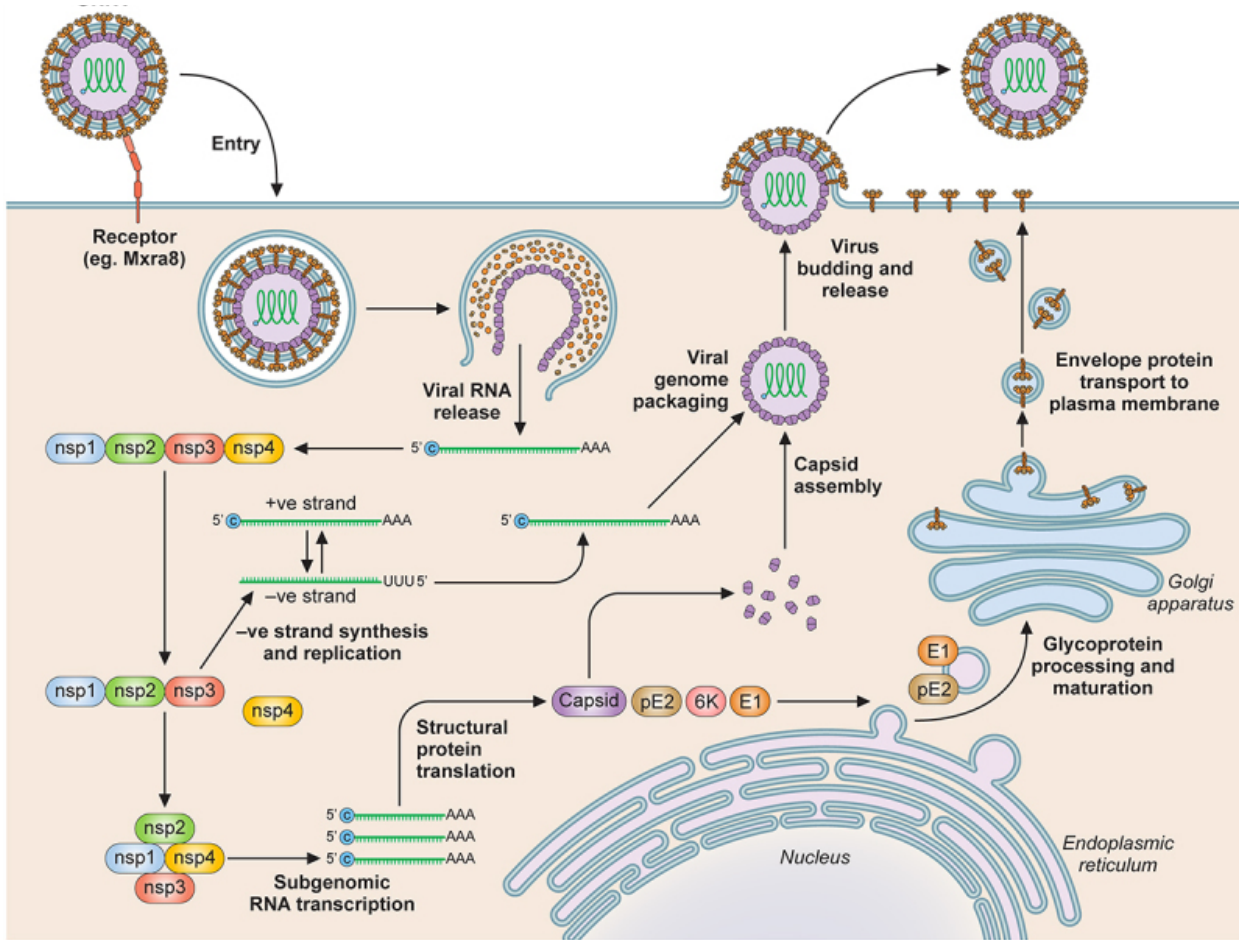


**Figure 2.** Diagram describing the replication cycle of ONNV, an Old-World Alphavirus that is highly similar to CHIKV. Diagram taken from Pathogenicity and virulence of O'nyong-nyong virus: A less studied Togaviridae with pandemic potential by Tong et al., 2024.

Most alphaviruses have a similar replication cycle as they share a highly conserved replication machinery, which is illustrated in the schematic drawn in **Figure 2** (Tong et al., 2024).

Once the virus releases its genetic material in the host cell, the first ORF is translated into the non-structural polyproteins as P1234, which is the precursor to the four non-structural

proteins (nsP1-4) and are essential for the viral replication machinery (Wang, Mahalingam, and Merits, 2025). nsP4 is the viral RNA-dependent RNA polymerase (RdRp), and its cleavage from P1234 by nsP2 protease is required for the activation of alphavirus RNA replication (Lello *et al.*, 2021). The presence of P123 stimulates the polymerase activity, and it is then cleaved by nsP2 protease to form other subunits that participate in viral RNA synthesis (Lello *et al.*, 2021). The efficiency of viral replication is dependent on the relative abundance of nsP4 (Lello *et al.*, 2021).

The early replicase, comprising the four nsPs, synthesizes a complementary negative strand RNA, which is then used to produce the 26S subgenomic RNA, as shown in **Figure 2** (Tong *et al.*, 2024). The subgenomic RNA then encodes for the second ORF, producing a single structural polyprotein C-E3-E2-6K/TF-E1 (Zimmerman *et al.*, 2023). This mechanism of using two open reading frames allows the viral replicase to produce large amounts of the subgenomic RNA, resulting in large quantities of structural proteins to be translated (Quetglas *et al.*, 2010). The host post-translational machinery, such as the ER and the Golgi apparatus, is then used to package all the viral components into a complete virion (Tong *et al.*, 2024).

## 1.3 Alphavirus entry and currently known host factor interactions

### 1.3.1 Versatility of alphavirus entry

Many studies have been carried out to identify various host receptors and entry factors that alphaviruses use for infection, yet there is still a limited understanding of viral entry. The E1 envelope glycoprotein is involved in cell fusion, while the E2 envelope glycoprotein binds to receptors and entry factors on the cell, facilitating viral entry via clathrin-dependent endocytosis (Basore *et al.*, 2019). However, another study has shown that CHIKV can efficiently enter and infect HEK-293T cells, which are genetically modified to silence clathrin using RNA interference to prevent clathrin-mediated endocytosis (Bernard *et al.*, 2010). In contrast to the previous study by Basore *et al.* (2019), the study by Bernard *et al.* (2010) seems to suggest that CHIKV entry does not require clathrin-dependent endocytosis but instead uses Eps15-dependent routes (Bernard *et al.*, 2010). The versatility in viral entry mechanisms complicates antiviral designs, as this functional redundancy would require therapeutic approaches that target post-endocytic steps or combine inhibitors that block multiple entry factors simultaneously. Thus, further research into alphavirus entry is required.

### 1.3.2 MXRA8

Matrix-remodeling associated protein 8 (MXRA8) is a cell-surface adhesion molecule with immunoglobulin-like domains. MXRA8 is known to be a key entry receptor for several arthritogenic alphaviruses, including CHIKV, RRV, ONNV, and Mayaro virus (MYRV). It

contains two Ig-like domains in a head-to-head orientation with a unique disulfide linkage structure (Song *et al.*, 2019). Cryo-EM at 4–5 Å carried out by Basore *et al.* (2019) revealed that alphaviruses, such as CHIKV, form a pocket with two adjacent E1-E2 heterodimers, facilitating the binding of alphaviruses to MXRA8 (Basore *et al.*, 2019). Another study by Zhang *et al.* (2018) used a genome-wide CRISPR/Cas9 based screen to identify if MXRA8 played a role in alphavirus infection. Single-clone MXRA8 knockouts in mouse 3T3 cells resulted in a reduction of infection by at least 90% for CHIKV, ONNV, MYRV, and RRV (Zhang *et al.*, 2018). When human or mouse MXRA8 cDNA is reintroduced to the knockout cells, viral entry and infection was fully restored, confirming that MXRA8 plays a role in alphavirus entry (Zhang *et al.*, 2018).

### 1.3.3 IRF3

Interferon Regulatory Factor 3 (IRF3) is a transcription factor that regulates cellular responses in various cell types, playing a crucial role in innate immunity (Yanai *et al.*, 2018). IRF3 directly regulates the transcription of several cytokine genes, including CXCL10, RANTES, interferon (IFN)-stimulated gene 56, IL-12p35, IL-15, and type I IFN genes (Yanai *et al.*, 2018), indicating that IRF3 plays a crucial role in host protection against pathogens. Upon recognition of viral RNA, through toll-like receptors in the host cells recognizing and binding to viral RNA, IRF3 is phosphorylated by either TANK-binding kinase 1 (TBK1) or inhibitor of NF-κB kinase ε/i (IKKε/i), resulting in the translocation of IRF3 into the nucleus, where it induces the transcription of type I IFN genes to activate innate immunity (Yanai *et al.*, 2018). Activation of IRF3 through CHIKV infection has been proven based on the phosphorylation and localization of IRF3 after CHIKV infection

(White *et al.*, 2010). IRF3 phosphorylation caused by CHIKV and the subsequent nuclear localization of IRF3 occurs between 8 and 16 h post-infection (White *et al.*, 2010). This makes IRF3 a potential target for host-directed therapeutics by enhancing IRF3 activation or downstream signaling for host resistance against alphavirus infections.

#### 1.3.4 Other receptors

Similar to MXRA8, the CD147 protein complex has been identified to be involved in CHIKV entry. The CD147 protein complex has five members: CD147, CD98, SLC1A5, ATP1A1, and ATP1B3 (De Caluwé *et al.*, 2021). CD147, like MXRA8, carries two immunoglobulin-like domains, and when CD147 was depleted, there was a minimal effect in reducing CHIKV infection (De Caluwé *et al.*, 2021). However, a double knockout of CD147 and SLC1A5, or CD98 and SLC1A5, lowered CHIKV infection (De Caluwé *et al.*, 2021). Interestingly, ONNV infection decreased when CD147 was knocked out, but not when both SLC1A5 and CD147 were knocked out (De Caluwé *et al.*, 2021). The difference in the set of receptors required to observe the reduction in infection between CHIKV and ONNV is unexpected, as the two viruses are highly similar alphaviruses with a genome conservation of 89% (Tong *et al.*, 2024).

The ATP synthase β subunit (ATPSβ) is a 50 kDa CHIKV-binding protein that has been identified through protein binding assays and co-immunoprecipitation studies, where antibodies against ATPSβ are used to obtain antibody-protein complexes probed with an antibody against the CHIKV E2 protein (Fongsaran *et al.*, 2014). Fongsaran *et al.* (2014)

demonstrated that the CHIKV E2 protein was specifically pulled down, indicating an interaction between CHIKV E2 and ATPS $\beta$  (Fongsaran *et al.*, 2014).

Prohibitin proteins (PHB) have multiple functions in the mitochondria but are also present in the plasma membrane (Wintachai P. *et al.*, 2012). When anti-PHB1 antibodies are added together with CHIKV to CHME-5 cells, the CHIKV infection rate is reduced, implying that PHB1 is involved in viral entry (Thuaud *et al.*, 2013; Wintachai P. *et al.*, 2012). Although neither PHB1 nor ATPS $\beta$  have the same high-affinity binding seen in MXRA8, they can still be used for viral entry by CHIKV, making them potential targets to inhibit CHIKV infection.

## 1.4 *Danio rerio* as a translational model

### 1.4.1 *Danio rerio* is an ideal whole-vertebrate model

*Danio rerio*, more commonly known as zebrafish, share roughly 70% of all human genes (Choi *et al.*, 2021), and almost 84% of known human disease-related genes have at least one zebrafish ortholog (Crouzier *et al.*, 2021). Zebrafish have several advantages over rodent animal models. A large experimental sample size can be obtained easily, as hundreds of embryos can be obtained in a single sitting (Choi *et al.*, 2021). Zebrafish also have low maintenance costs, as they have minimal housing requirements (Crouzier *et al.*, 2021). Generating crispant zebrafish is significantly faster and cheaper compared to using mouse models (Crouzier *et al.*, 2021). Crispants are mosaics composed of wild-type and

mutant cells, achieved by CRISPR/Cas9 genetic engineering technology, creating a mixture of wild-type and targeted gene knockouts within the animal (Keeley *et al.*, 2025). The optically transparent bodies of zebrafish also allow researchers to track fluorescently labelled viruses or immune cells during infection (Sofyantoro *et al.*, 2024).

#### 1.4.2 Disadvantages of using *Danio rerio* as an animal model

While zebrafish possess functional neutrophils and macrophages, the adaptive immune system of the larvae does not fully mature until 3-6 weeks post-fertilization (Franza *et al.*, 2024). As such, embryonic studies only capture the innate immune system response to infection. Additionally, zebrafish have a more limited immunoglobulin class profile, including IgM, IgG, and IgZ/T, compared to the human IgM, IgG, IgE, IgA, and IgD (Franza *et al.*, 2024). This makes embryonic zebrafish a limiting model for evaluating vaccine efficiency (Franza *et al.*, 2024).

#### 1.4.3 Rapid genetic modification of *Danio rerio*

Genes in zebrafish can be easily disrupted by injecting embryos at the single-cell stage with a pre-assembled CRISPR-associated protein (Cas9) ribonucleoprotein complex (Hoshijima *et al.*, 2019). The Cas9 system proceeds through three molecular steps (Mengstie and Wondimu, 2021). The first step is recognition, where a 20-nucleotide recognition site found within the guide RNA (gRNA) forms complementary base pairs with the target sequence (Mengstie and Wondimu, 2021). Without the gRNA, the Cas9 protein is inactive (Mengstie and Wondimu, 2021). The Cas9 enzyme scans the double-stranded

DNA for a protospacer-adjacent motif (PAM), 5'-NGG-3', where N is any nucleotide. Upon recognition of PAM, local DNA melting occurs, allowing the gRNA to pair with the complementary gene of interest to form an RNA-DNA hybrid (Mengstie and Wondimu, 2021). However, the mechanism by which Cas9 melts the DNA is not fully understood yet (Mengstie and Wondimu, 2021). The second step is cleavage, where the successful base pairing of the gRNA and DNA triggers conformational changes that activates two of the CRISPR/Cas9's nuclease domains, namely the HNH and RuvC domains (Mengstie and Wondimu, 2021). The HNH domain is named after its catalytic site, which contains a His-Asn-His sequence (Mengstie and Wondimu, 2021). The HNH domain cuts the strand that hybridizes with the gRNA, while the RuvC endonuclease domain cleaves the opposite strand, producing a blunt double-end strand break, which is exactly three nucleotides upstream of the PAM (Mengstie and Wondimu, 2021). The final step of the Cas9 system is to repair, where the blunt double-end strand break is sealed via error-prone non-homologous end joining carried out by the host machinery (Mengstie and Wondimu, 2021). This leads to random insertions or deletions of a few bases, also known as indels, causing a shift in the reading frame (Mengstie and Wondimu, 2021). Since the reading frame has changed, a different amino acid sequence is encoded, which changes the structure of the protein and leads to an expected loss of function. Multiple gRNAs can be co-injected to carry out precise domain deletion (Mengstie and Wondimu, 2021). The speed and scalability of the CRISPR/Cas9 system are among the main reasons why zebrafish are used over mouse models, especially for preliminary studies.

Moreover, zebrafish's high fecundity, external fertilization, rapid development, and small size also make them extremely useful for genetic manipulation experiments (Parvez, Brandt, and Peterson, 2023). Crispants are able to mimic stable knockout models with an indel efficiency of over 88%, eliminating the need to breed full knockout zebrafish, which requires two generations of adult animals that are homozygous for the mutant alleles and therefore limits the efficiency and affordability of genetic screens (Debaenst *et al.*, 2024). Furthermore, knockout of specific genes might be lethal for the zebrafish later during development, resulting in those fish not reaching adulthood, making it impossible to obtain two generations of adult animals that are homozygous for the mutant alleles. Using crispants in the embryonic stage allows for greater survivability for experiments.

## 1.5 Knowledge gap and study rationale

Currently, most receptors and host factors involved in alphavirus interaction have been identified using immortalized human or rodent cell lines, where the genes of interest are either depleted or overexpressed (De Caluwé *et al.*, 2021; Fongsaran *et al.*, 2014; Thuaud *et al.*, 2013; White *et al.*, 2010; Wintachai P. *et al.*, 2012; Yanai *et al.*, 2018; Zhang *et al.*, 2018). These systems cannot determine whether viral entry is dependent on a single receptor, such as MXRA8, or on multiple factors working together, including other cellular systems and receptors, to facilitate viral entry. They are also incapable of demonstrating whether viral interactions with host factors, such as IRF3, can be disrupted when other systems are involved. Interactions with various complex biological systems can only be observed through live animal models such as zebrafish or mice. By testing full-length

knockouts of genes, such as MXRA8 and IRF3, this gap can be closed, bringing targeted antivirals against alphaviruses a step closer to reality.

Additionally, preliminary research conducted in the lab suggested that the RdRp of Virus X may contribute to the localization of the virus to the swim bladder (*Unpublished Data*). This observation suggests that there may be host factors found in the tissues surrounding the swim bladder that interact with the RdRp of Virus X. It also indicates that this host factor interaction occurs beyond viral entry, as the RdRp of Virus X is not part of the external structure of the virus. This observation introduces a novel mechanism of host-virus interaction, as viral tropism was previously considered to be governed by structural proteins. However, more data is required to prove this relationship.

## 1.6 Project objectives

The primary aim of this study is to assess the relationship between MXRA8, IRF3, and the infectivity of alphaviruses, particularly CHIKV and Virus X, in an *in vivo* zebrafish model. Through CRISPR/Cas9-mediated gene editing, this study aims to evaluate how the disruption of either MXRA8A, which is the zebrafish ortholog of MXRA8 in humans, or IRF3 influences viral infection and host response. It also seeks to understand the observed differential tropism of alphaviruses caused by the RdRp of Virus X in zebrafish. By identifying key domains in host factors that modulate alphavirus infection, potential therapeutic targets can be identified for the development of targeted antivirals.

## 2. Methods and materials

### 2.1 Zebrafish maintenance and preparation

Wild-type AB strain zebrafish (*Danio rerio*) were housed in an aquarium system with recirculating water at Proteos facility under the care of the Institute of Molecular and Cell Biology, Agency for Science and Technology Research. Embryos were obtained through natural spawning. Embryos were maintained in E3 PTU supplemented with methylene blue (made using 50x E3 stock [1.46% (w/v) of NaCl, 0.063% (w/v) of KCl, 0.243 % (w/v) of CaCl<sub>2</sub>.H<sub>2</sub>O, 0.407% (w/v) of MgCl<sub>2</sub>.6H<sub>2</sub>O] and 20x PTU water stock [0.06% (w/v) PTU (Sigma Aldrich, Cat no. P7629)]). Once the larvae were 2 days post-fertilization (dpf), they were transferred to E3 PTU (without methylene blue).

## 2.2 Evaluating the difference in alphavirus infection between Crispant Zebrafish

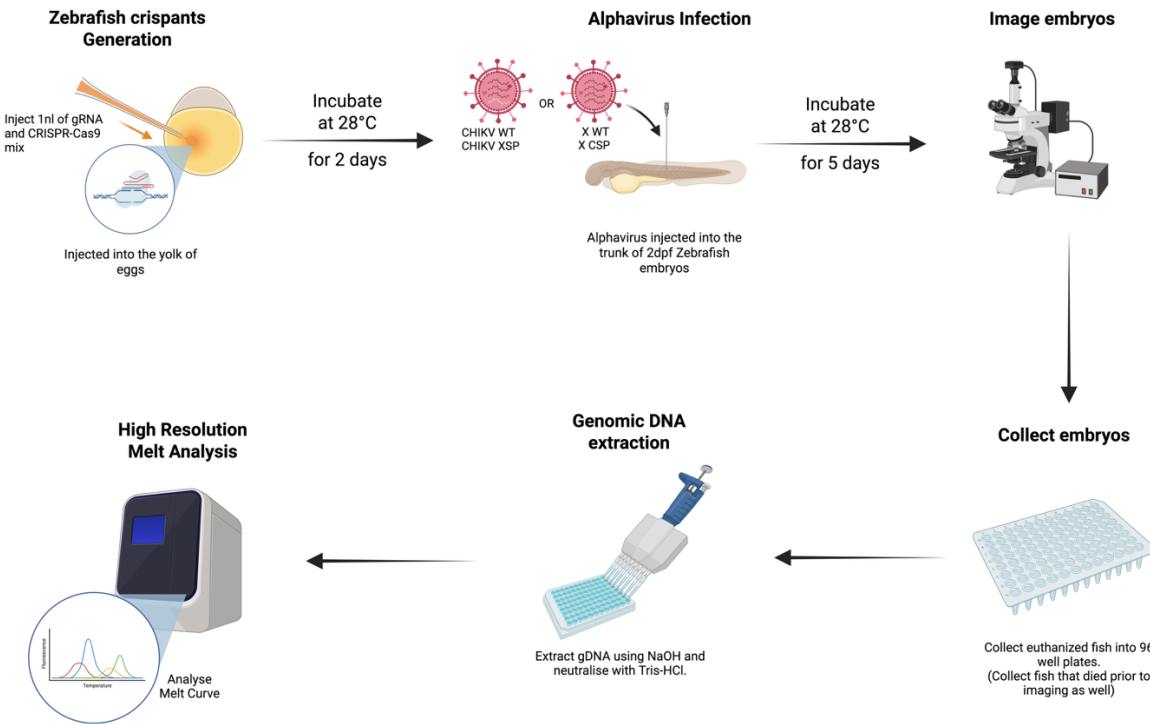


**Figure 3.** A schematic diagram that overviews the experimental plan to evaluate whether the presence or absence of specific genes causes upregulation or downregulation of alphavirus infection.

### 2.2.1 Knockout zebrafish generation via CRISPR/Cas9 technology

Crispant zebrafish with the genes MXRA8A or IRF3 knocked out were generated using CRISPR/Cas9-mediated genome editing. Each solution used to carry out gene depletion was composed of 2 µL of gRNA that targets the gene of interest, 0.323 µL of Alt-R™ S.p HiFi Cas9 protein (IDT, Cat No. 1081061), 1.677 µL of nuclease-free water, and 1 µL of

0.5% phenol red dye (Sigma-Aldrich, Cat No. P0290-100ML). As a control, some embryos at the single-cell stage were injected with scrambled (scram) gRNA, which does not target any gene. The gRNAs used are listed in **Table 1**. Approximately 1 nL of the mixture was injected into the yolk of single-cell embryos using a glass needle pulled from glass capillaries with a micropipette puller. Injection volume was calibrated using a micrometer slide. The embryos were then incubated at 28°C in E3 PTU water supplemented with methylene blue. Dechorionation of the eggs was performed at one dpf using a 1:10 dilution of 10 mg/mL pronase (Sigma-Aldrich, Cat No. P5147). The dechorionated embryos were then washed and incubated at 28°C in fresh E3 PTU water.

**Table 1.** gRNA sequences used for CRISPR/Cas9

MXRA8_target_1	5' TAATACGACTCACTATAGGCTGGATTACTCGAAGGTTTAGAGCTAGAAATAGC 3'
MXRA8_target_2	5' TAATACGACTCACTATAGGGTTTCTCTCAGCTCGTAGTTTAGAGCTAGAAATAGC 3'
MXRA8_target_3	5' TAATACGACTCACTATAGGGCGTGCACCCGGTTAGAGCTAGAAATAGC 3'
MXRA8_target_4	5' TAATACGACTCACTATAGGAGCTTACTGTGAGCCCTCGTTAGAGCTAGAAATAGC 3'
IRF3_target_1	5' TAATACGACTCACTATAGGCAGTGCTTCGCGCTAAGTTAGAGCTAGAAATAGC 3'
IRF3_target_2	5' TAATACGACTCACTATAGGAAGGTGCTCGTGGTTAGAGCTAGAAATAGC 3'
IRF3_target_3	5' TAATACGACTCACTATAGGTTGGAGAACGACTCGTTAGAGCTAGAAATAGC 3'
IRF3_target_4	5' TAATACGACTCACTATAGGATTCACGGCACCGTTAGAGCTAGAAATAGC 3'
Scram_1	5' TAATACGACTCACTATAGGCAGGAAAGAATCCCTGCCGTTAGAGCTAGAAATAGC 3'
Scram_2	5' TAATACGACTCACTATAGGTACAGTGGACCTCGGTGTCGTTAGAGCTAGAAATAGC 3'
Scram_3	5' TAATACGACTCACTATAGGCTTCATAACATAGACGATGGTTAGAGCTAGAAATAGC 3'
Scram_4	5' TAATACGACTCACTATAGGCGTTGCAGTAGGATCGGTTAGAGCTAGAAATAGC 3'

## 2.2.2 Virus strains and fluorescent reporters

Viruses used in this study include wild-type Chikungunya virus (CHIKV WT), Chikungunya virus expressing the structural proteins from Virus X (CHIKV XSP), Wild-type Virus X (X WT), and Virus X with Chikungunya structural proteins (X CSP). All viral strains are genetically engineered to express the ZsGreen fluorescent reporter, enabling the tracking of infection via fluorescence microscopy based on the green signal produced. The viruses are diluted in 0.5% phenol red dye before injection, to visualize the injection process and aid in calibrating the injection volume. Dilution varied for each virus based on optimal signal-to-toxicity balance. CHIKV WT is diluted 1:4 (2 µL of virus with 8 µL of dye). X WT is diluted 1:4 (2 µL of virus with 8 µL of dye). CHIKV with the structural proteins of Virus X is diluted 2:1 (2 µL of virus with 1 µL of dye). X with structural proteins of CHIKV is diluted 1:1 (2 µL of virus with 2 µL of dye).

## 2.2.3 Infection of zebrafish larvae

Two days post-fertilization, the embryos were anesthetized using 0.4% tricaine solution (prepared by dissolving 0.4 g of tricaine powder [Sigma-Aldrich, Cat No. A5040] in 100 mL RO water). The larvae were grouped into 6-well plates and transferred to shallow glass wells for injection. A foot pedal-controlled microinjector using pressurized nitrogen gas was used to inject 1 nL of diluted virus into the trunk of the zebrafish using a glass needle. The embryos were incubated at 28°C in fresh E3 PTU water after injection.

## 2.2.4 Fluorescence imaging of infected zebrafish

Five days post-infection (dpi), the infected larvae were anesthetized and mounted on the inverted lid of a 6-well plate using 2.5% methylcellulose (prepared by dissolving 2.5 g of methylcellulose [Sigma-Aldrich, Cat No. M0512] in 100 mL of RO water). Larvae were aligned laterally, with their eyes stacked on top of each other and their heads positioned to the left, to maintain a consistent imaging orientation. The crispant zebrafish and scram zebrafish were then transferred to a 96-well plate with one zebrafish per well to be euthanized for High Resolution Melt (HRM) analysis.

Fluorescence imaging was performed using a fluorescence stereomicroscope with a blue light filter to detect ZsGreen expression. Images were analyzed using Fiji (also known as ImageJ) to quantify the intensity of fluorescence, which is correlated to the infection burden. The fluorescence was measured by setting a threshold to remove any background fluorescence based on the uninfected control zebrafish. The analyzed data were plotted on GraphPad Prism.

Due to the non-parametric nature of the dataset, a two-tailed Mann-Whitney U test ( $\alpha = 0.05$ ) was carried out to compare the scram and crispants zebrafish that were infected with the same virus to determine statistical significance ( $p < 0.05$ ).

## 2.2.5 High Resolution Melt (HRM) analysis

For genotype validation of the crispant, HRM is conducted on the genomic DNA (gDNA) from each larva that was injected with gRNA targeting a gene or scram gRNA. The gDNA is first extracted using 50 µL of 50 mM NaOH (prepared from 5 M NaOH [Sigma-Aldrich, Cat No. S8263]). The samples are then incubated at room temperature for 10 minutes, followed by incubation at 95°C for 10 minutes, and immediately transferred to ice for 2 minutes. Neutralization of NaOH is then carried out by adding 5 µL of 1 M Tris-HCl [Bio Basic, Cat No. USD8137] to each well. The gDNA is then diluted with 120 µL of Nuclease-Free Water in each well. The diluted gDNA is used as the template for a 10 µL HRM reaction using the Precision Melt Supermix (Bio-Rad, Cat No. 172-5112). HRM was performed using a qPCR thermocycler using standard cycling conditions and protocol provided by the manufacturer. The primers used for the HRM analysis are listed in **Table 2**.

**Table 2.** Primers used for HRM analysis

MXRA8A_fwd	5' CAGGCTAAAAGACCGTCAGC 3'
MXRA8A_rev	5' ATACGTCCCTGGTTGTAGCC 3'
IRF3_fwd	5' TGGAGATCCGTCTGTGTGGA 3'
IRF3_rev	5' GCAGAATGAGGATCGGAGGG 3'

## 2.3 Determine if protein D of Virus X results in swim bladder localization of alphaviruses.

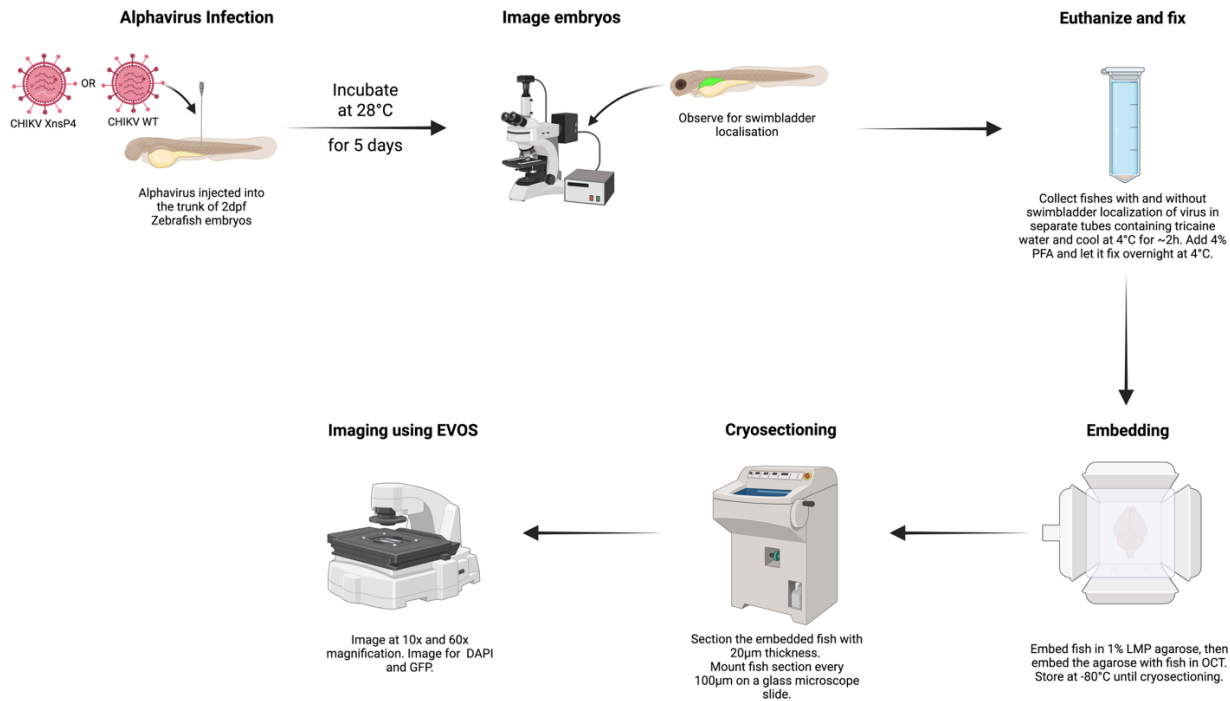


**Figure 4.** A schematic diagram that overviews the entire experimental plan to evaluate if the RdRp of Virus X results in swim bladder localization of alphaviruses.

### 2.3.1 Infecting zebrafish with alphaviruses

Viruses used include wild-type Chikungunya virus (CHIKV WT) and CHIKV expressing the RdRp from Virus X (CHIKV XnsP4). All viral strains were genetically engineered to express the ZsGreen fluorescent reporter. The viruses are diluted in 0.5% phenol red dye. CHIKV WT is diluted 1:4 (2 µL of virus with 8 µL of dye), CHIKV XnsP4 is diluted 1:9 (2 µL of virus with 18 µL of dye). The zebrafish embryos were collected as mentioned in **Section 2.1**. They were then infected using the procedure detailed in **Section 2.2.3**.

### 2.3.2 Fluorescence imaging of infected zebrafish

Five dpi, the infected larvae were anesthetized and mounted on the inverted lid of a 6-well plate using 2.5% methylcellulose. Larvae were aligned laterally, with their eyes stacked on top of each other and their heads positioned to the left, to maintain a consistent imaging orientation. Fluorescence imaging was performed using a fluorescence stereomicroscope with a blue light filter to detect ZsGreen expression. Positive swim bladder localization of the virus was observed and documented. Images were analyzed using Fiji to quantify the intensity of fluorescence, which is correlated to the infection burden. The fluorescence was measured by setting a threshold to remove any background fluorescence based on the uninfected control zebrafish. The analyzed data were plotted on GraphPad Prism. The larvae were then euthanized and fixed overnight in 4% paraformaldehyde (prepared from Pierce 16% Formaldehyde (w/v) [Thermofisher Scientific, Cat No. 28906]).

### 2.3.3 Cryosectioning and immunofluorescence

The fixed larvae were washed three times in PBS (Gibco, Cat No. 10010023), and cryoprotected in 30% sucrose (Bio Basic, Cat No. SB0498) for 24-48 hours. The larvae were then embedded by suspending them in 1% low-melting point agarose (Promega, Cat No. V2111). The set agarose with the zebrafish head facing down towards the bottom of the mold was then submerged in Optimal Cutting Temperature (OCT) compound (Sakura Finetek, Cat No. 25608-930) over dry ice. The molds were frozen at -80°C for at least 24 hours to set. 20 µm transverse sections of the zebrafish were cut using a cryostat and mounted onto a glass slide. The mold was allowed to warm to -20°C, which is the optimal temperature for sectioning to prevent curling of sections (Liyanage *et al.*, 2017). The sections were then washed three times with PBS before the nuclei were stained with VECTASHIELD® Antifade Mounting Medium with DAPI (Vector Laboratories, Cat No. H-1200). Slides containing the sections were then imaged using an EVOS microscope with images taken using brightfield, GFP, and DAPI filters. The number of zebrafish that had swim bladder localization of the virus was analyzed using a chi-square or Fisher's exact test at  $\alpha = 0.05$  to determine if there is a significant association between the virus strain used and the presence of swim bladder localization.

### 3. Results

#### 3.1 Swim bladder localization caused by CHIKV XnsP4 compared to CHIKV WT

Previous work in the laboratory group has shown that the RdRp of Virus X may be contributing to the localization of the virus to the swim bladder (*Unpublished Data*). Hence, we aimed to assess the precise localization of the virus in that organ.

Wild-type AB strain zebrafish were used to assess the localization pattern of CHIKV XnsP4 virus compared to CHIKV WT virus. A total of seventeen embryos were infected with CHIKV WT, while another seventeen embryos were infected with CHIKV XnsP4.

**Figure 5** shows a column graph comparing the fluorescence intensity, which represents the viral infection burden of either CHIKV WT or CHIKV XnsP4. Not all control zebrafish are visible, as zebrafish with zero fluorescence signal cannot be plotted on a log scale.

### Alphavirus infection in AB zebrafish (Experiment 1)

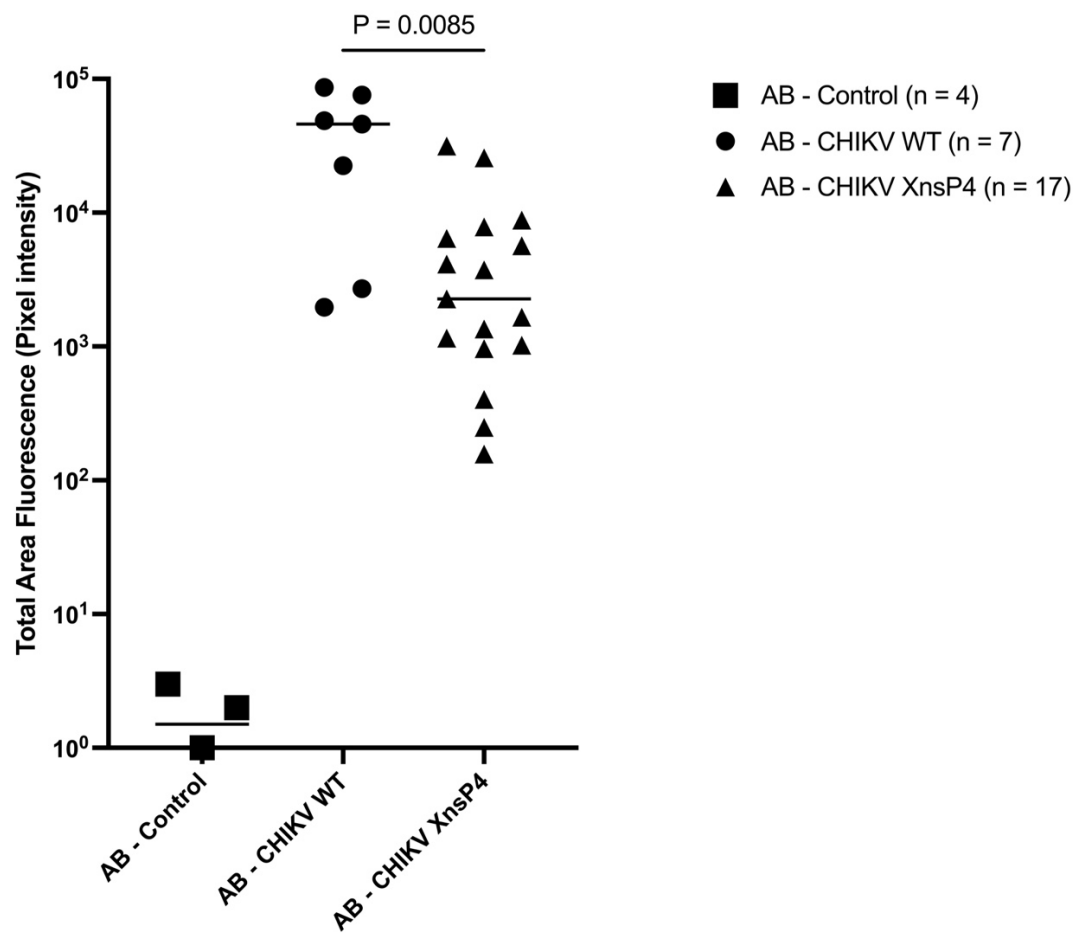


**Figure 5.** Quantification of CHIKV WT and CHIKV XnsP4 infection in wild-type AB zebrafish based on the intensity of ZsGreen fluorescence.

As shown in **Figure 5**, the p-value obtained from the Mann-Whitney U test was 0.0085, which is below the significance level of 0.05, indicating a statistically significant difference between the infection burdens of CHIKV WT and CHIKV XnsP4. Although the purpose of this experiment is not to compare the infection burden between the two viruses, but rather to assess the localization of the virus in the swim bladder, it is notable that the fluorescence intensity of CHIKV XnsP4 is significantly lower than that of CHIKV WT. This could indicate that a lower volume of virus than required was injected or that the virus was controlled by the zebrafish better.

Notably, there was a high fatality rate of 58.8% from the CHIKV WT virus, where ten out of seventeen fish had died. Improper techniques such as piercing the zebrafish multiple times, handling the zebrafish roughly during injection, and causing the yolk to burst are some of the likely causes of mortality in the zebrafish. On the other hand, no mortality was observed in the CHIKV XnsP4 infected group. This might be due to the group being injected later; hence, rough handling of the zebrafish was reduced, as it became more comfortable to handle the zebrafish.

The imaged embryos were fixed overnight and sectioned into 20  $\mu\text{m}$  slices via cryosectioning. Stained sections were imaged using the EVOS microscope, as shown in **Figures 6 and 7**.

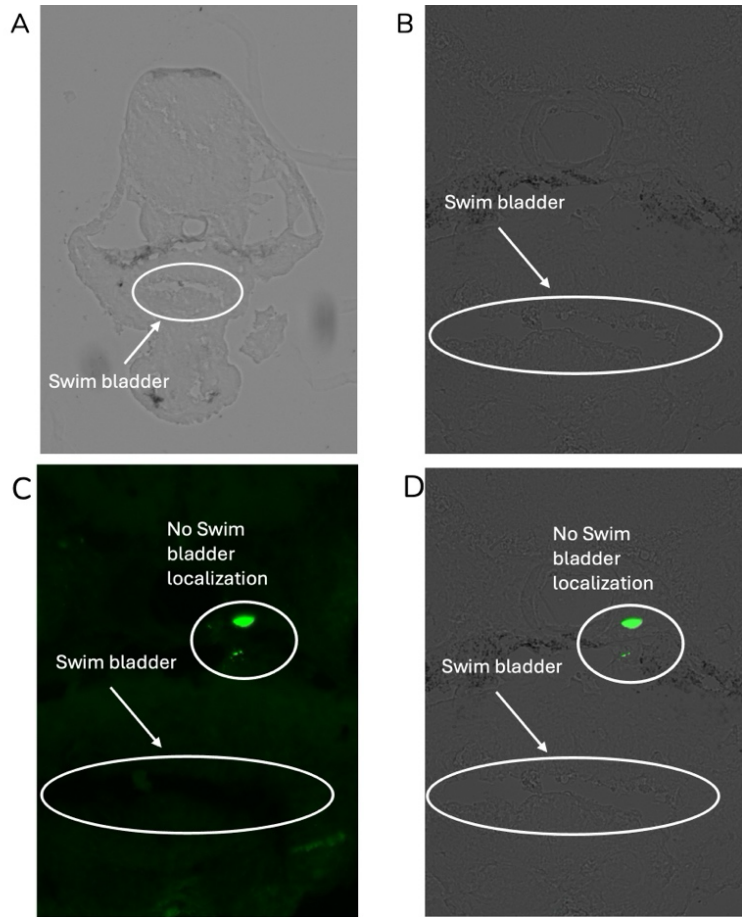


**Figure 6.** Images of transverse sections of zebrafish infected with CHIKV WT. (A) is the brightfield image of a section of zebrafish infected with CHIKV WT at 10X magnification. (B) is the brightfield image of a section of zebrafish infected with CHIKV WT at 60X magnification. (C) is the GFP image of a section of zebrafish infected with CHIKV WT at 60X magnification. (D) is the merged image of both brightfield and GFP images.

**Figure 6** shows the transverse section of zebrafish infected with CHIKV WT. The brightfield image seen in **Figure 6A** was used to identify the swim bladder region. A book, *An Interactive atlas of Zebrafish Vascular Anatomy*, was used as a reference to aid in histological identification. After identifying the swim bladder, the section was magnified to 60x, and the filter was changed to observe ZsGreen fluorescence.

From **Figures 6C and 6D**, the green reporter signal from CHIKV WT was observed away from the swim bladder, in the notochord, which suggests an absence of swim bladder localization. The viral infection is expected to be around the notochord as it is located near the trunk, which is the site of injection.

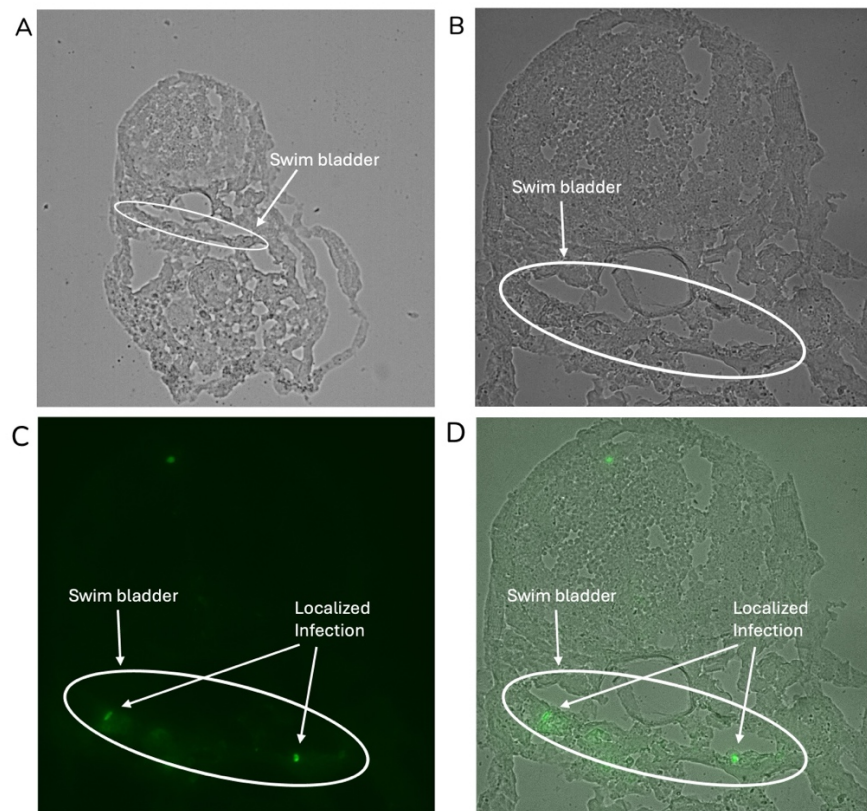


**Figure 7.** Images of transverse sections of zebrafish infected with CHIKV XnsP4. (A) is the brightfield image of a section of zebrafish infected with CHIKV XnsP4 at 10X magnification. (B) is the brightfield image of a section of zebrafish infected with CHIKV XnsP4 at 60X magnification. (C) is the GFP image of a section of zebrafish infected with CHIKV XnsP4 at 60X magnification. (D) is the merged image of both brightfield and GFP images.

**Figures 7C and 7D** show the transverse sections of zebrafish infected with CHIKV XnsP4. The green reporter signal is observed in the tissue surrounding the swim bladder, suggesting that CHIKV XnsP4 is being localized to the swim bladder. **Figure 8** compares the proportion of swim bladder localization of each virus observed.

**Proportion of zebrafish observed with  
swim bladder localization of virus  
(Experiment 1)**

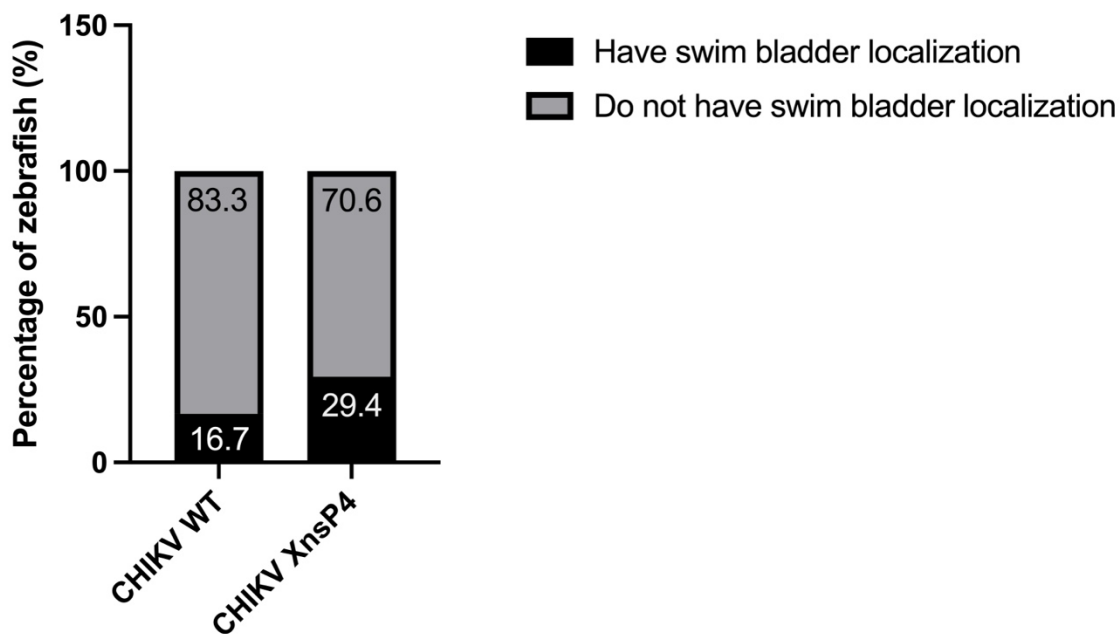


**Figure 8.** Comparison of the proportion of swim bladder localization of virus observed between CHIKV WT and CHIKV XnsP4 in Experiment 1.

Fisher's Exact test was performed to analyze the relationship between swim bladder localization of the virus and the virus used for infection, to determine if there was a significant difference in the swim bladder localization of the virus between the two groups. The p-value obtained was 0.6287, which is higher than the significance threshold ( $p < 0.05$ ), so it can be concluded that there is no significant relationship between the swim bladder localization of the virus and the virus used to infect this group of zebrafish.

### 3.1.1 Optimizing zebrafish injection techniques

The experiment was then repeated with modifications to the techniques used during injection. Five embryos were infected with CHIKV WT, while another five embryos were infected with CHIKV XnsP4. Instead of navigating the zebrafish from a point near the yolk, the tail end and head were instead used to arrange and hold the zebrafish in place. This was done to prevent accidental puncture of the yolk sac, which will lead to the death of the zebrafish. Additionally, the needle angle was adjusted to prevent the needle from being too steep, thereby avoiding complete penetration of the larva, which could also contribute to the death of the fish.

To increase the CHIKV XnsP4 signal from the zebrafish, a larger volume of the virus was used for infection by increasing the injection pressure. **Figure 9** shows a column graph comparing the fluorescence intensity between the CHIKV WT and CHIKV XnsP4 obtained from the repeated experiment. Not all control zebrafish are visible, as zebrafish with zero

fluorescence signal cannot be plotted on a log scale. Some zebrafish infected with CHIKV XnsP4 also could not be plotted on a log scale due to a lack of fluorescence signal.

### Alphavirus infection in AB zebrafish (Experiment 2)

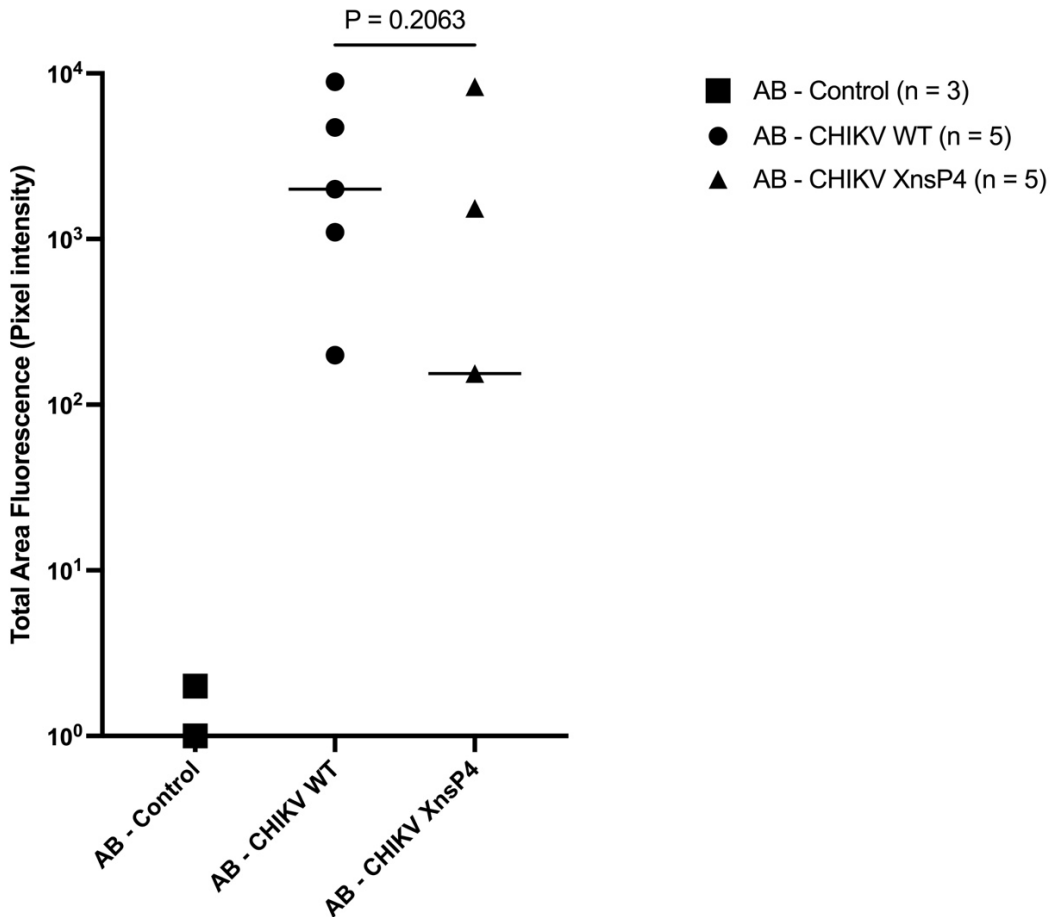


**Figure 9.** Quantification of CHIKV WT and CHIKV XnsP4 infection (Experiment 2) in wild-type AB zebrafish based on the intensity of ZsGreen fluorescence

In the repeat, the fatality rate is now zero, with all five fish infected per group surviving. This shows that the modification made to the injection techniques has prevented unnecessary deaths of the zebrafish due to suboptimal injection techniques. Additionally, there are some improvements to the viral burden of CHIKV XnsP4. As shown in **Figure 9**, there is no longer a significant difference in fluorescence intensity between the two viruses, as the p-value is 0.2063, which is above the significance level of 0.05.

However, the median fluorescence intensity of CHIKV XnsP4 is still lower than that of CHIKV WT, and there are also some zebrafish that seemed to lack the ZsGreen signal entirely, suggesting that the tube of virus used may be losing its reporter or its infectivity. Another possible explanation is that this group of zebrafish was able to clear the infection more easily due to a potentially stronger immune system.

Because the optimization used a small sample size, and some zebrafish lacked measurable infection signal for CHIKV XnsP4, the swim bladder localization was assessed using fluorescence microscopy, but cryosectioning was not carried out. **Figure 10** compares the proportion of swim bladder localization of each virus observed.

### Proportion of zebrafish observed with swim bladder localization of virus (Experiment 2)

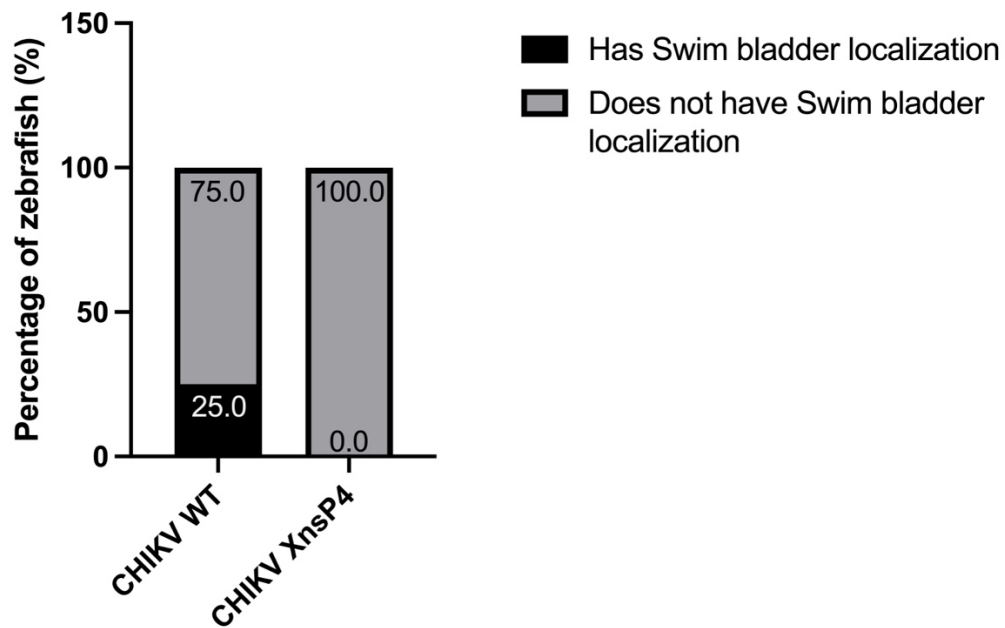


**Figure 10.** Comparison of the proportion of swim bladder localization of virus observed between CHIKV WT and CHIKV XnsP4 in Experiment 2.

As seen in **Figure 10**, there was no swim bladder localization observed in the CHIKV XnsP4 infected zebrafish; this is likely due to an issue with the virus. Fisher's Exact test was carried out to analyze the relationship between swim bladder localization of the virus and the virus used to infect, determining if there was a significant difference in the localization of the virus between the two groups. Since the p-value obtained was greater than 0.9999, it can be concluded that there is no significant association between the swim bladder localization of the virus and the virus used to infect the group of zebrafish.

### 3.1.2 Optimizing CHIKV XnsP4 infection

The experiment was then repeated using a new tube of CHIKV XnsP4 virus to determine if the unexpected results observed previously were due to an issue with the virus in the previous experiment. Additionally, a larger sample size of 10 zebrafish per virus was used to carry out statistical tests with higher accuracy. **Figure 11** presents a column graph comparing the fluorescence intensity between the CHIKV WT and CHIKV XnsP4 obtained from the repeated experiment with a larger sample size. Not all control zebrafish are visible, as zebrafish with zero fluorescence signal cannot be plotted on a log scale. **Figure 12** compares the proportion of swim bladder localization of each virus observed.

### Alphavirus infection in AB zebrafish (Experiment 3)

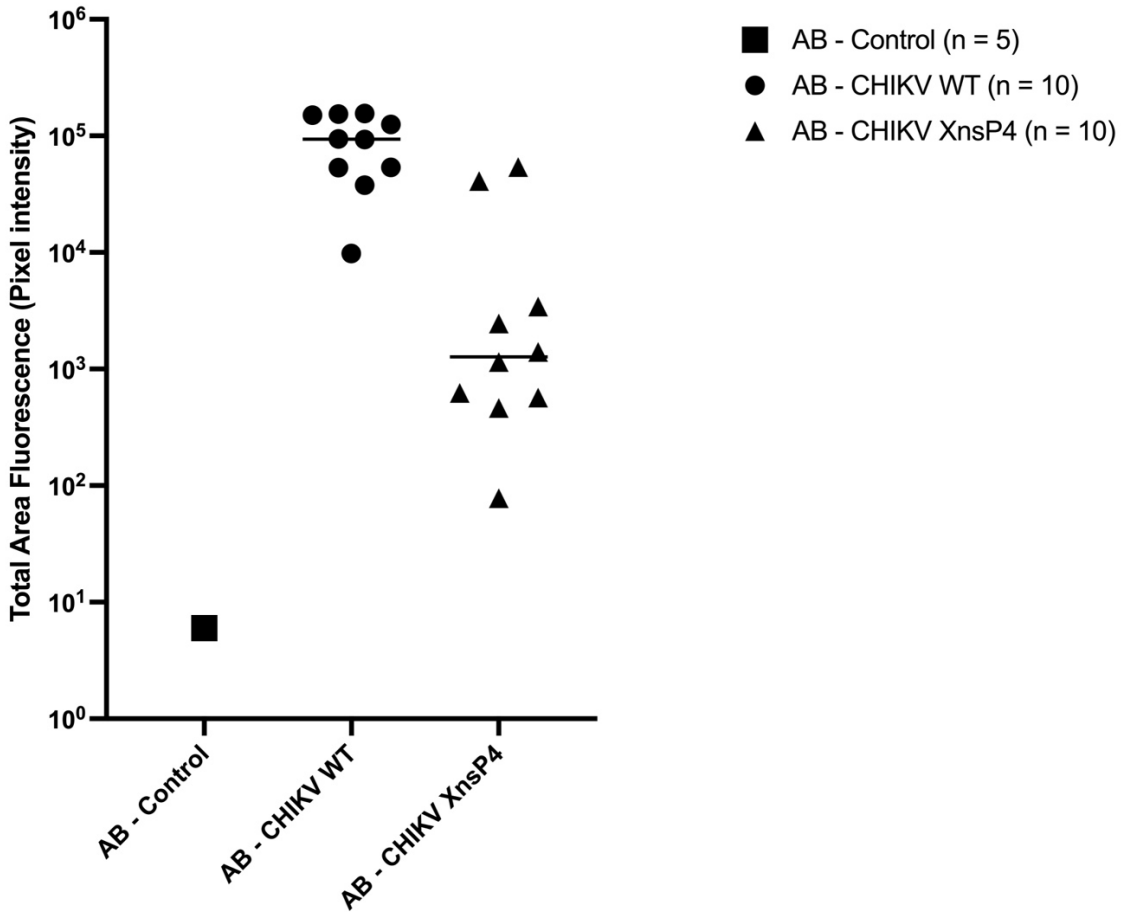


**Figure 11.** Quantification of CHIKV WT and CHIKV XnsP4 infection (Experiment 3) in wild-type AB zebrafish based on the intensity of ZsGreen fluorescence

In this repeat, the fatality rate remained zero, with all ten fish infected per group surviving. CHIKV XnsP4 fluorescence signal remained low. The virus concentration was ruled out as a contributing factor, as injections carried out in other experiments using the same virus dilution for CHIKV XnsP4 exhibited a strong signal. The injection technique was also unlikely to be the issue, as CHIKV WT had consistently demonstrated a good signal, and the same technique was used for both viruses. Further troubleshooting and optimization are required.

### Proportion of zebrafish observed with swim bladder localization of virus (Experiment 3)

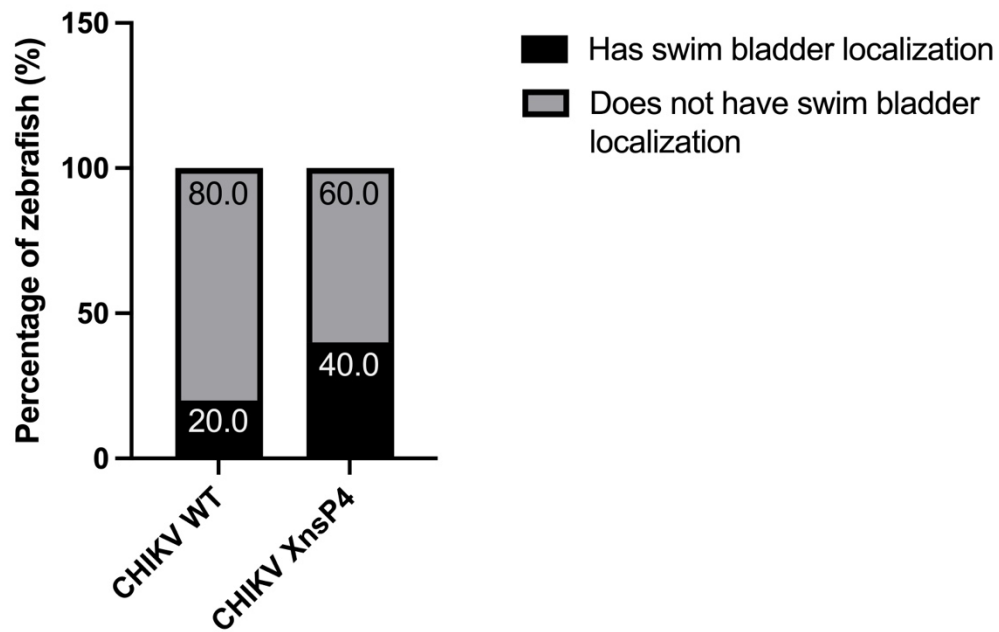


**Figure 12.** Comparison of the proportion of swim bladder localization of viruses observed between CHIKV WT and CHIKV XnsP4 in Experiment 3.

Fisher's exact test was conducted to analyze the relationship between swim bladder localization of the virus and the virus used for infection, to determine if there was a significant difference in localization between the two groups. Since the p-value obtained was 0.6285, which is higher than the significance level, it can be concluded that there is no significant relationship between the swim bladder localization of the virus and the virus strain used to infect. However, CHIKV XnsP4 was observed to have twice the number of fish exhibiting swim bladder localization than CHIKV WT, suggesting the presence of a trend that could not be statistically significant due to the small sample sizes.

### 3.1.3 Consolidation of swim bladder localization results

To perform a cross-experimental analysis, swim bladder localization data from the first and third experiments were consolidated into **Figure 13**, and Fisher's exact test was carried out to determine if there were any significant associations between swim bladder localization of the virus and the virus strain used for infection. The second experiment was omitted due to outliers caused by the possible issue with the CHIKV XnsP4 virus or the zebrafish having an abnormally stronger immune response to infection. The p-value obtained was 0.3125, which is higher than the significance level. It can be concluded that there is no significant relationship between the virus localization to the swim bladder and the virus strain.

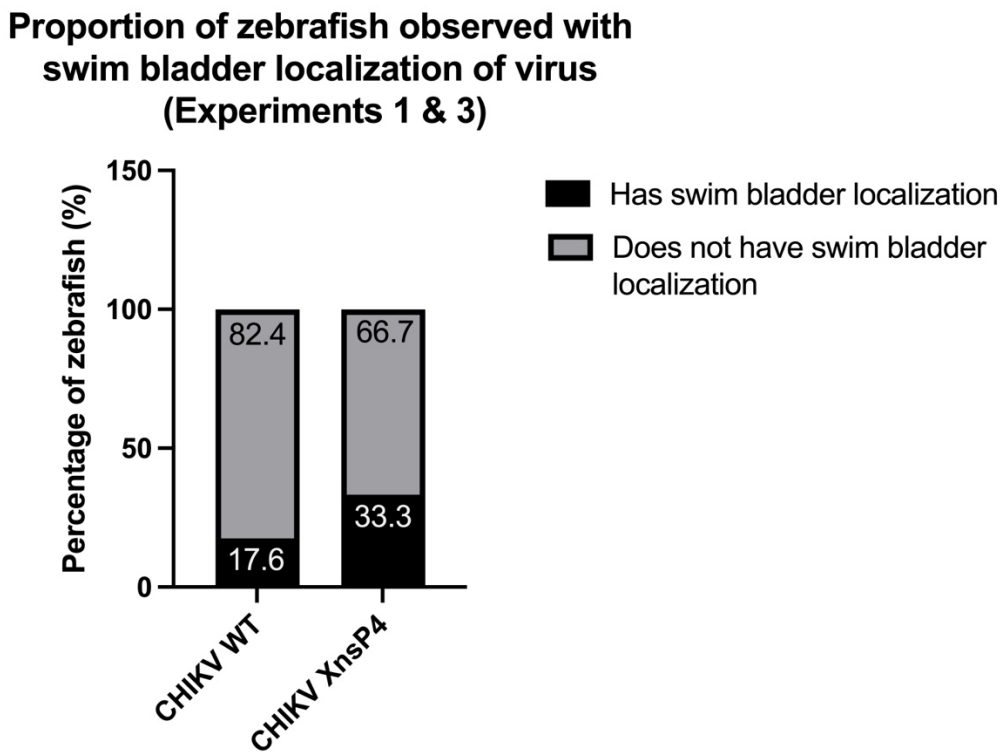


**Figure 13.** Comparison of the proportion of swim bladder localization of virus observed between CHIKV WT and CHIKV XnsP4 across Experiments 1 & 3.

### 3.2 Genetic depletion of MXRA8A and IRF3 affects alphavirus infection in zebrafish

Most alphavirus host factors have been identified using immortalized human or rodent cell lines, which do not capture the complexity of *in vivo* interactions. These *in vitro* systems are unable to show if host factor-virus interactions, whether before, during, or after viral entry, are affected when multiple, complex systems work together. Such interactions with various complex biological systems can only be studied through live animal models.

Hence, to investigate host factors of alphavirus infectivity, zebrafish eggs at the single-cell stage were injected with CRISPR/Cas9 reagents targeting either MXRA8A (zebrafish ortholog of MXRA8) or IRF3, along with scrambled (scram) gRNA, which does not target any genes and serves as a control. The crisprants and control zebrafish were infected with four different genetically engineered virus constructs expressing a ZsG reporter, CHIKV WT, X WT, CHIKV XSP, and X CSP. The infected larvae were then imaged at five dpi using a fluorescence stereomicroscope with a blue light filter, which excites ZsG.

The fluorescence intensity of the ZsG reporter was then quantified using Fiji software to determine viral burden. The data was plotted using GraphPad Prism software, and a statistical analysis was carried out using two-tailed Mann-Whitney U tests ( $\alpha = 0.05$ ).

### 3.2.1 Effect of MXRA8A in alphavirus infection in zebrafish

**Figure 14** shows a column graph comparing the fluorescence intensity between the zebrafish injected with scram gRNA or MXRA8A-targeting gRNA to create crisprants. The scram zebrafish will theoretically still express MXRA8A since the scram gRNA does not target any known genes, and thus, the CRISPR/Cas9 system should not deplete any genes.

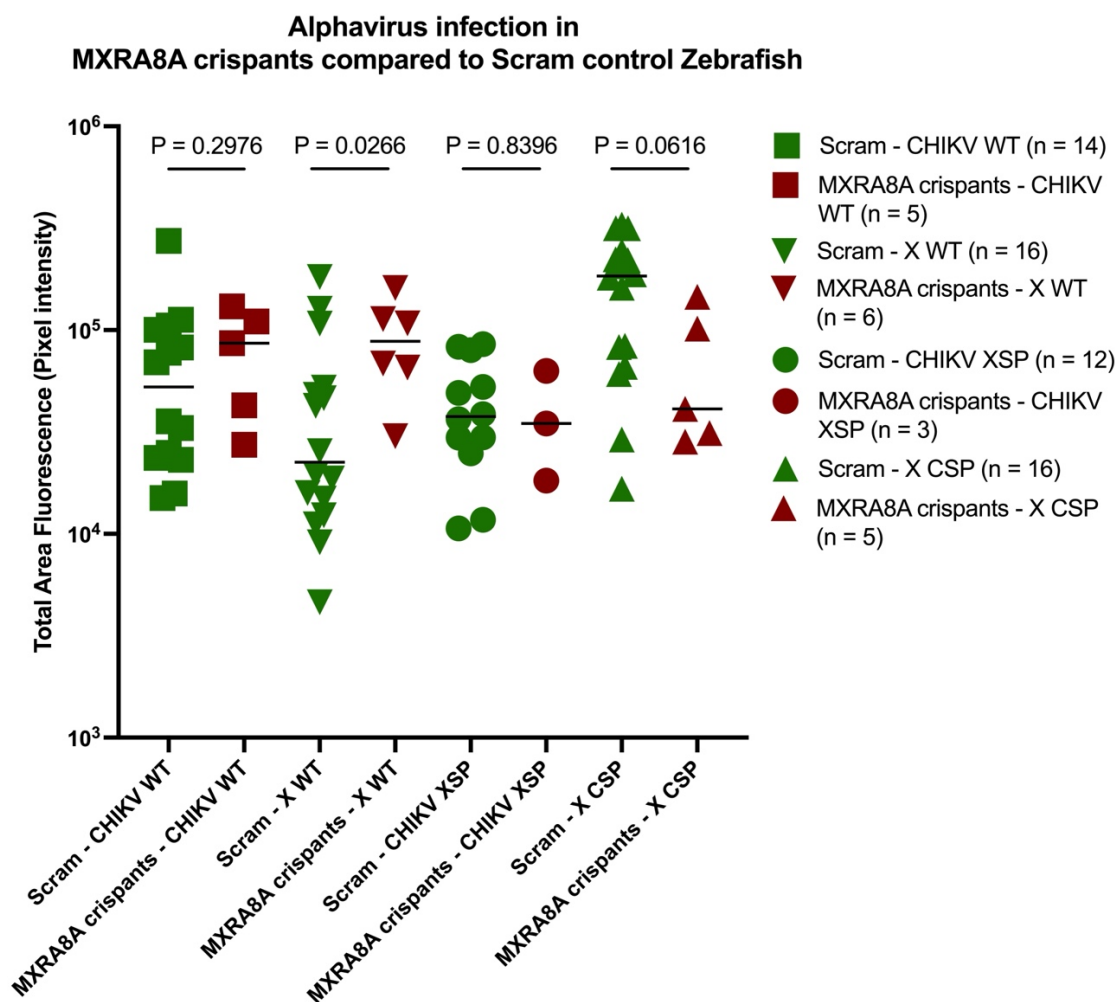


**Figure 14.** Quantification of Alphavirus Infection in MXRA8A crisprants compared to scram control zebrafish based on the intensity of ZsGreen fluorescence.

Each data point represents an individual zebrafish, and the horizontal lines represent the median fluorescence for each group. Medians were used instead of means due to the presence of outliers in many groups.

A statistically significant increase in fluorescence intensity was observed in MXRA8A crispants zebrafish infected with X WT compared to the scram zebrafish infected with the same virus. The p-value obtained from the Mann-Whitney U test was 0.0266, which is below the significance level of 0.05, indicating a statistically significant difference between the two groups. Based on the median fluorescence, it can be deduced that depleting MXRA8A leads to an increase in infection of X WT.

However, there was no significant difference in signal intensity observed between the MXRA8A crispants and scram zebrafish infected with CHIKV WT, CHIKV XSP, or X CSP. The p-values were, respectively, 0.2976, 0.8396, and 0.0616, which are higher than the significance level of 0.05. It is interesting to note that the p-value for the difference in signal intensity between MXRA8A crispants and scram zebrafish infected with X CSP is 0.0616, which is close to the significance threshold of 0.05, suggesting a potential difference in viral infection when the MXRA8A receptor is missing that is driven by the X nsPs. Based on the median fluorescence, X CSP appears to reduce viral infection when the MXRA8A receptor is absent. However, more data points are required to determine the statistical significance of this observation.

### 3.2.2 Effect of IRF3 in alphavirus infection in zebrafish

**Figure 15** shows a column graph comparing the fluorescence intensity between the scram zebrafish and IRF3 crisprants. The scram zebrafish were expected to retain IRF3 expression as the scram gRNA does not target any genes, and thus, the CRISPR/Cas9 system should not deplete any genes.

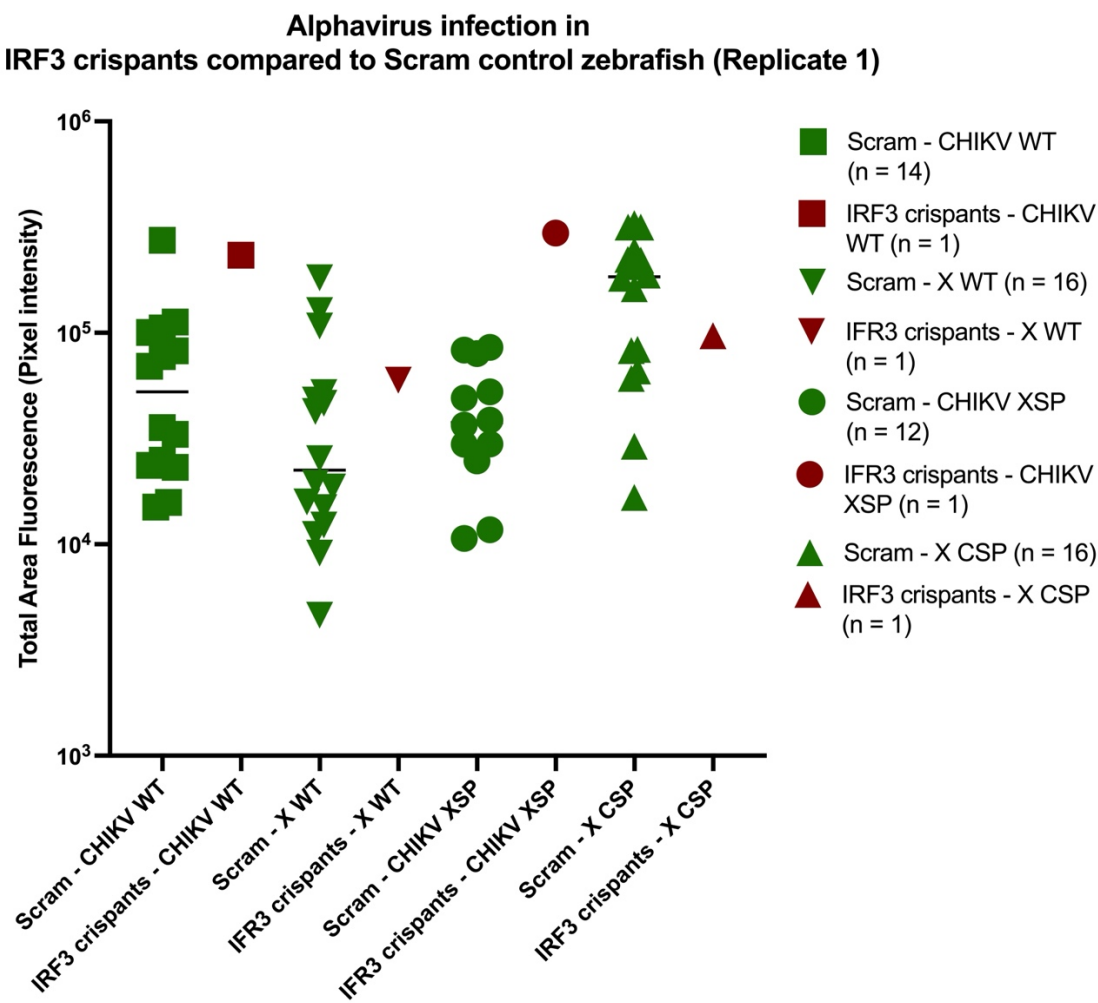


**Figure 15.** Quantification of alphavirus infection in IRF3 crisprants compared to scram control zebrafish (Replicate 1) based on the intensity of ZsGreen fluorescence

Each data point represents an individual zebrafish, and the horizontal lines represent the median fluorescence for each group.

Unfortunately, the majority of the IRF3 crispants zebrafish had died before they could be infected with alphavirus. As such, only two zebrafish per group could be infected, with one per group dying after infection, resulting in only one data point per experimental group. This resulted in insufficient data points for statistical analysis to be conducted. Hence, the experiment was repeated to produce more data points. **Figure 16** shows a column graph of the repeated experiment, comparing the fluorescence intensity between the scram zebrafish and IRF3 crispants.

**Alphavirus infection in  
IRF3 crisprants compared to Scram control Zebrafish (Replicate 2)**

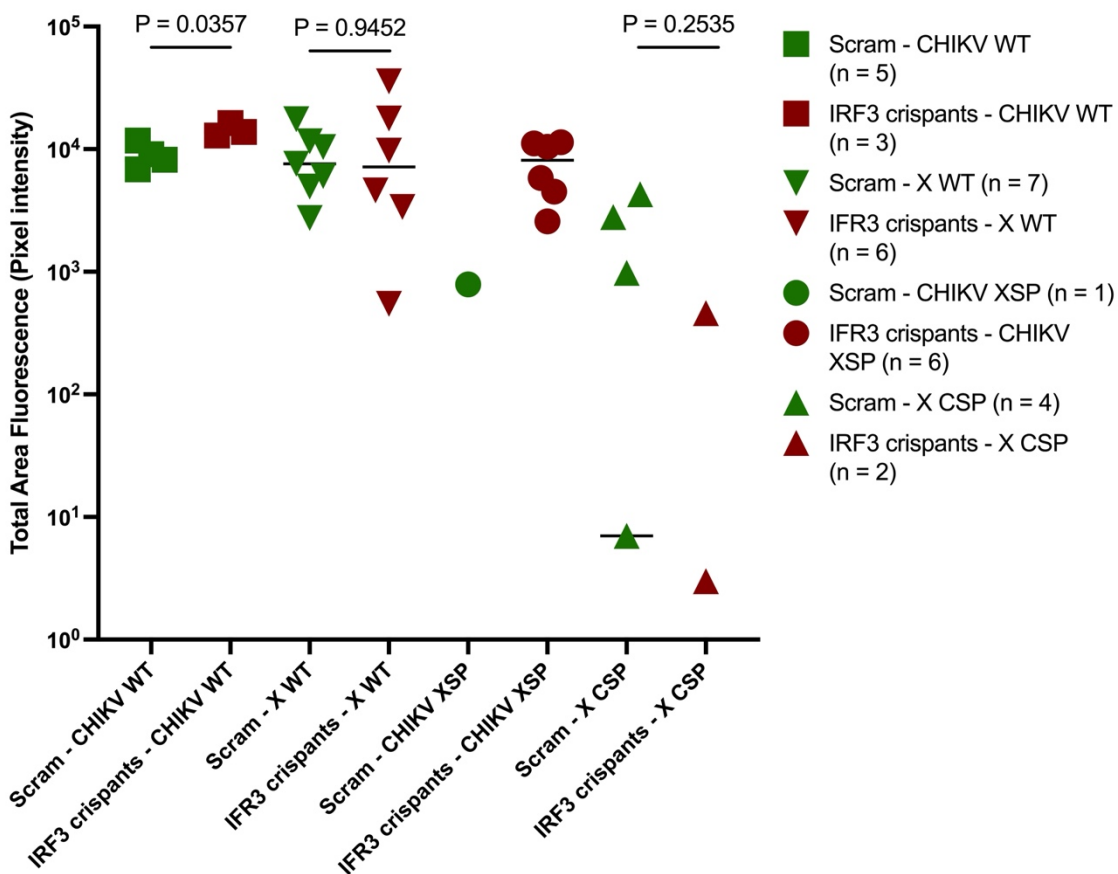


**Figure 16.** Quantification of alphavirus infection in *IRF3* crisprants compared to scram control zebrafish (Replicate 2) based on the intensity of ZsGreen fluorescence.

A statistically significant increase in fluorescence intensity was observed in *IRF3* crisprants zebrafish infected with CHIKV WT compared to the scram zebrafish. The p-value obtained from the Mann-Whitney U test was 0.0357, which is below the significance level of 0.05, indicating a statistically significant difference between the two groups. Based on the median fluorescence, it can be deduced that depleting *IRF3* leads to an increase in

infection of CHIKV WT. Notably, 50% of the IRF3 crispants zebrafish were found to be dead following CHIKV WT infection.

There was no significant difference in signal intensity observed between the IRF3 crispants and scram zebrafish infected with X WT. The p-value was 0.9452, which is higher than the significance level.

CHIKV XSP resulted in the death of 6 out of 7 scram zebrafish while all the IRF3 crispants zebrafish survived. Due to this, there was only one data point for the scram zebrafish infected with CHIKV XSP. As such, it was not possible to perform a statistical test due to insufficient data. This unexpected death rate could be due to an overdose of tricaine during anesthetization prior to infection. Although the same concentration of tricaine was added, that group of zebrafish could have been left in the tricaine water for too long before they were changed to fresh E3 PTU water.

X CSP also does not seem to be affected by the presence or absence of IRF3, as the p-value was 0.2535, which is higher than the significance level. However, it is notable that a few of the scram (three out of seven) and IRF3 crispant zebrafish (five out of seven) seem to have died, possibly due to an overdose of tricaine. Since IRF3 is a key host signaling factor, the lack of any difference in infectivity for both X CSP and X WT seems to suggest that the non-structural proteins of Virus X do not interact with IRF3.

### 3.2.3 High Resolution Melt analysis of crispant zebrafish

To validate the successful knockout of MXRA8A and IRF3 genes in the zebrafish, High Resolution Melt (HRM) analysis was performed using the genomic DNA extracted from each larva. The HRM technique can be used to distinguish wild-type, heterozygous, and mutant genotypes. Melting temperature and curve shape are both used to identify sequence differences (*What is High Resolution Melting (HRM)?*, 2025). **Figure 17** displays the melt and difference curve of both MXRA8A HRM (**Figures 17A and 17B**) and IRF3 HRM (**Figures 17C and 17D**) analyses.

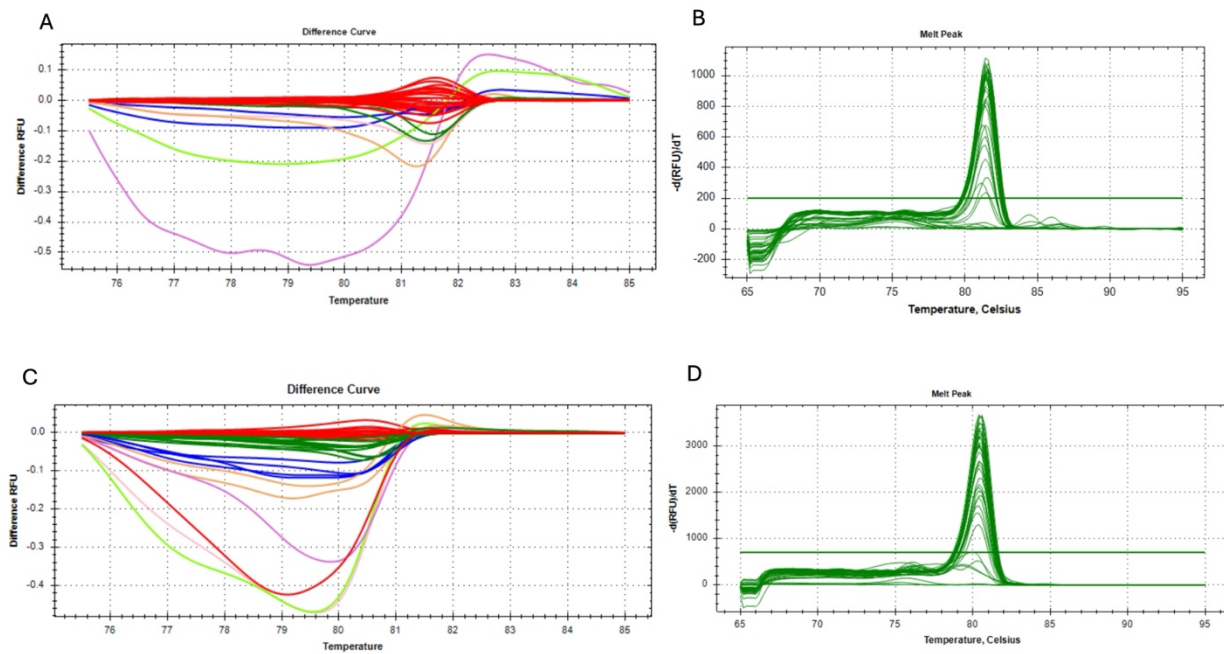


**Figure 17.** Difference and Melt curves generated after HRM Analysis. (A) is the difference curve generated from MXRA8A crispants, scramble zebrafish (positive control), and NTC. (B) is the melt curve generated from MXRA8A crispants, scramble zebrafish (positive control), and NTC. (C) is the difference curve generated from IRF3 crispants, scramble zebrafish (positive control), and NTC. (D) is the melt curve generated from IRF3 crispants, scramble zebrafish (positive control), and NTC.

Ideally, two distinct clusters should be observed. One cluster of melting temperatures represents the zebrafish that have the respective genes knocked out, and another cluster of melting temperatures that represents the zebrafish that can still express the respective genes. The different clusters are annotated with different colors in the difference curve plots. As shown in **Figures 17A and 17C**, there are many different clusters for both the MXRA8A crisprants zebrafish HRM analysis and the IRF3 crisprants zebrafish HRM analysis respectively, which may indicate an issue with the HRM primers. Likely, they are not specific to the target sequence that was removed using CRISPR, leading to the amplification and detection of non-specific, undesired fragments. Thus, these HRM results cannot be used for the validation of gene knockout. Redesign and optimization of primers is necessary.

## 4. Discussion

This study aimed to gain a deeper understanding of the interactions between alphaviruses and their host factors using zebrafish as an animal model. By generating targeted crisprants of host receptors and factors using the CRISPR/Cas9 genetic engineering technology, the importance and effects of these receptors and factors on the infectivity of alphaviruses can be better understood. Chimeric viral strains produced from genetic modification to contain viral proteins from a different alphavirus were used to determine the effect and significance of specific viral proteins on virus infection. By understanding these key host factor-virus interactions, a potential therapeutic target could be identified. While this study was focused on Chikungunya virus and Virus X, the findings may be relatable to other alphaviruses.

### 4.1 Tropism of chimeric CHIKV XnsP4 virus

Preliminary lab observations had suggested that the RNA-dependent RNA polymerase (RdRp) of Virus X might be responsible for the localization of the virus to the swim bladder of the zebrafish. This observation suggests the presence of host factors in the tissues surrounding the swim bladder that are capable of interacting with the RdRp of Virus X. Since the RdRp is responsible for viral replication and is not part of the structure of the virus, it shows that host factor-protein interaction goes beyond viral entry. This challenged the current understanding of viral tropism, which is currently known to be governed by structural proteins. However, more data is required to establish if the viral tropism caused

by the RdRp of Virus X is statistically significant. Hence, the research started with the infection of wild-type AB strain zebrafish embryos with both CHIKV WT and CHIKV XnsP4.

Earlier experiments resulted in a significant amount of sample loss due to technical errors, including multiple piercings of the zebrafish, rough handling during injection, and the yolk bursting. During the first run of the experiment shown in **Figure 5**, 58.8% of the zebrafish infected with CHIKV WT were found to be dead. This is due to human error, as the dilution of the virus used had been optimized not to cause death. As Beck, Watt, and Bonner have described previously, any damage to the yolk will result in rapid embryonic death (Beck, Watt, and Bonner, 2014). This is because the yolk sac of zebrafish embryos houses a supply of proteins, lipids, and micronutrients to sustain essential metabolic function (Sant and Timme-Laragy, 2018). The technique used to infect the zebrafish needs to be optimized to avoid causing injury or death to the zebrafish, as this will interfere with the analysis that can be made, falsely increasing the fatality and effect of the virus. The injection technique was modified to use other parts of the zebrafish, such as the head or the tail, to position and prepare it for injection. Through the optimization of techniques, a reliable method was established, resulting in 0 deaths, as shown in the later experimental repeats illustrated in **Figures 9 and 11**.

The infected zebrafish were viewed under a fluorescence microscope to observe the ZsG reporter signal, where swim bladder localization was noted. To validate and observe

which part of the swim bladder the virus is localizing to, the infected zebrafish were sliced into transverse sections via cryosectioning. However, during the first run, the slices kept curling, rendering them unusable as the tissues rolled onto themselves. This observation was caused by the OCT block being too cold prior to cutting (*Immunofluorescence protocol for frozen sections*, 2025). Sumedha Liyanage *et al.* (2017) have found that the temperature of the specimen plays a significant role in obtaining a straight, perfect slice. The optimal temperature was found to be -20°C (Liyanage *et al.*, 2017). As such, the OCT blocks were allowed to warm to -20°C in the cryostat before sectioning for subsequent experiments. Additionally, applying gentle thumb pressure to warm the block face aided in obtaining a flat and clean slice.

Across two experiments, as shown in **Figure 13**, 17.6% of CHIKV WT infected zebrafish were observed with swim bladder localization of the virus. In contrast, 33.3% of CHIKV XnsP4 infected zebrafish were observed with swim bladder localization of the virus. Although statistical analysis shows that this observation is statistically insignificant, the lack of significance could be attributed to the small sample size. Due to difficulty in natural spawning, the number of healthy eggs that could be obtained during the course of these experiments was not sufficient to perform the experiments with a larger sample size.

The observation of CHIKV XnsP4 leading to a higher occurrence of swim bladder localization has sparked interest, as tissue tropism is thought to be controlled by surface glycoproteins of the virus interacting with host receptors (Li *et al.*, 2021). However, in this case, swim bladder localization of the virus seems to be caused by a protein that is not involved in the structure of the virus. RdRp is a non-structural protein and may play a role in controlling host cell signaling and exploiting different components of stress granules to increase replication in a way that favors the virus in specific organs of the zebrafish, such as in the tissues surrounding the swim bladder (Kim *et al.*, 2016; Treffers *et al.*, 2023).

It also suggests that the viral nsPs may play a role beyond viral replication. A possible hypothesis would be that RdRp interacts with certain host factors found in the cells within the tissues surrounding the swim bladder, which can increase the permissivity of the virus into the cell, creating the tropism observed. This observation challenges the current understanding of the alphavirus genome, proteins, and their functions. If studied further, new discoveries could open up new pathways and novel ideas for the development of therapeutic targets in science.

## 4.2 MXRA8A and IRF3 crispants zebrafish affect the infectivity of certain alphaviruses in zebrafish

Previous literature has shown that MXRA8 is an entry receptor for CHIKV and various other alphaviruses, thereby having a proviral effect on CHIKV infection (Zhang *et al.*, 2018). Similarly, it was previously found that IRF3 is a key host immune signaling factor that is activated by CHIKV (White *et al.*, 2010). IRF3 has been shown to have an antiviral effect on CHIKV infection as it leads to the production of IFN- $\alpha/\beta$  (Rudd *et al.*, 2012). However, those studies were carried out in cell lines and not living models with complex pathways. As a result, this study was conducted to determine whether the zebrafish orthologs of MXRA8 and IRF3 exhibit the same essential interaction with CHIKV, Virus X, and their chimeric viruses containing structural protein swaps in a live animal model setting. It is crucial to determine if host factor-pathogen interactions remain true *in vivo*, as multiple systems working together may alter the interactions between the virus and host factors. Evidence suggests that *in vitro* studies often inadequately reflect the complexity of *in vivo* systems (Díaz-Pascual *et al.*, 2017). Hence, MXRA8A and IRF3 depleted zebrafish crispants were generated using CRISPR/Cas9 gene editing technology.

As shown in **Figure 14**, the presence or absence of MXRA8A did not significantly affect the infection burden of CHIKV WT. This differs from existing literature. Based on the literature, the expected observation would be to see significantly reduced viral infection in the MXRA8A crispants zebrafish, as it would suggest that without MXRA8A, CHIKV

WT is unable to enter and infect cells efficiently. The lack of significant reduction in CHIKV WT infection suggests that MXRA8A is not as essential as once perceived when used in a complex system like a whole animal, as there may be other host receptors that interact with CHIKV WT, allowing it to enter and infect cells. Interestingly, when the zebrafish were infected with X WT, the signal intensity of the crispants was significantly higher than that of the scram zebrafish. This suggests that MXRA8A may have antiviral properties against Virus X or act as a binding/entry inhibitor. For example, MXRA8A may cause steric hindrance of other receptors that play a role in Virus X infection. However, repeats of the experiment are required along with a larger sample size for confirmation.

Curiously, the structural protein swaps of both viruses, CHIKV XSP and X CSP, do not show any significant difference in infectivity. This suggests that the infectivity of the virus is not only dependent on the structural genes but also on the non-structural genes. Although X WT and CHIKV XSP have the same structural proteins and will therefore interact with receptors the same way, CHIKV XSP did not exhibit the same infectivity pattern as X WT. CHIKV XSP lacks the non-structural proteins of Virus X, and this observation suggests that the difference seen in X WT infectivity is not due to just the structural proteins alone.

Additionally, when X CSP, which contains the non-structural proteins of X but not the structural proteins, was used to infect, there was still no significant difference in viral burden between the crispants and scram groups. This suggests that the difference seen

in X WT infectivity is also not due to the non-structural proteins alone. From that, we can conclude that host-pathogen interaction is not just between the structural glycoproteins and host receptors, but the non-structural proteins appear to play a role. A possible hypothesis would be that the non-structural proteins of Virus X interact with factors in the host cell, allowing the structural proteins of Virus X to interact with different receptors more efficiently, leading to an increase in its infectivity. Further studies should be conducted to determine which host factors are interacting with different virus factors beyond surface receptors.

Since IRF3 is an essential regulator of the immune system, there were issues in generating enough crispant zebrafish, as it led to a higher mortality rate. IRF3 is a transcription regulator that regulates the expression of various genes critical for innate immunity. Presence of bacteria or microbes in the needles, plates, E3 PTU water, or the fish facility used to house these crispants could have led to the death of the embryos, as they have a deficient innate immune system and lack adaptive immunity at that stage of life. Without innate immunity, the pathogens could lead to a rapid spread of infection, overwhelming the body, and leading to the early death of the embryos. To overcome this issue, a larger number of embryos at the single-cell stage were injected so that an appropriate sample size of IRF3 crispant zebrafish could be obtained.

As shown in **Figure 16**, IRF3 crispant zebrafish infected with CHIKV WT have a significantly higher signal intensity, which is representative of viral infectivity. This is consistent with existing knowledge as IRF3 has been shown to be essential for innate immunity since it controls the transcription of various cytokine genes (Yanai *et al.*, 2018). CHIKV has been shown to be able to activate IRF3, leading to the initiation of an innate immune response to suppress CHIKV infection (White *et al.*, 2010). Since the virus infectivity is increased in the absence of IRF3, it can be concluded that IRF3 is an antiviral factor and plays a critical role in controlling CHIKV WT infection.

However, like MXRA8, the signal intensity of all the other recombinant viruses was not affected by the presence or absence of IRF3, which brings the interesting question of why the other chimeric viruses, one of which has the structural proteins of CHIKV, and another has the non-structural proteins of CHIKV, are not able to replicate the effect caused by CHIKV WT. It also raises the question of how and at what level CHIKV WT interacts with IRF3. A possible hypothesis to explain this phenomenon would be that the nsPs of Virus X can interact and inhibit IRF3, and thus, the presence or absence of IRF3 does not make a difference. Hence, the crispants did not see any increase or decrease in infection when infected with X WT and X CSP. The experiment should be repeated for CHIKV XSP, as the lack of a sufficient sample size prevented statistical analysis from determining the effect of IRF3 on CHIKV XSP infectivity.

In order to validate the genotypes of the zebrafish and ensure that the genes of interest have been knocked out, all infected zebrafish were collected, regardless of whether they died before imaging at five dpi or remained alive to the conclusion of the experiment. Surviving zebrafish at five dpi were euthanized prior to collection. The collected zebrafish then have their genomic DNA (gDNA) extracted to be used as the template for High Resolution Melt (HRM) analysis. Sequence differences are identified based on the melting temperature and the melt curve. Similar melt profiles, which represent similar sequences, are grouped. Ideally, only two clusters should be seen, which are the cluster with a melt curve for zebrafish that still expresses the targeted gene and a separate cluster with a melt curve for zebrafish that have the genes knocked out. However, as can be seen from **Figure 17**, the HRM analysis carried out resulted in multiple clusters.

Marcin Słomka *et al.* (2017) had faced a similar issue. It was said that there may be a genetic variation within the sequence complementary to the primer, which leads to incorrect clustering due to the amplification of the wrong sequence. It was also noted that shorter amplicon length had led to an improved clustering (Słomka *et al.*, 2017). Based on this, the problem of too many clusters is likely due to inadequate primer design. The primers should be redesigned to accurately determine the genotype of the zebrafish. It is essential to determine and validate the genotype of the zebrafish to associate the increase or decrease in viral infectivity with the presence or absence of the gene, which is the primary objective of this study.

The main limitation of this study is the lack of a sufficient sample size. Due to an inability to obtain zebrafish eggs via natural spawning, experiments could only be performed on a limited number of zebrafish. Moreover, due to a lack of available zebrafish larvae, experiments could not be repeated easily to validate the trend being observed and ensure it was not a random occurrence. Another important limitation of this study to note is the inability to verify the genotypes of crispant zebrafish. Due to the primers being unoptimized, the results obtained could not be analyzed.

## 5. Conclusion and future work

In conclusion, this study used zebrafish as an *in vivo* model to investigate the roles of MXRA8, a key alphavirus entry receptor, and IRF3, a key host signaling factor, during alphavirus infection. Crispant zebrafish targeting these genes were generated using CRISPR/Cas9 gene editing technology. Using these crisprants, it was discovered that MXRA8A exhibits an antiviral effect against X WT, but not CHIKV WT, despite previous identification as a CHIKV entry receptor. While knockdown of IRF3 exhibits an expected antiviral effect against CHIKV WT, it did not have any effect against X WT.

The findings suggest that host-virus interactions may require the involvement of both structural and non-structural viral proteins. Additionally, preliminary evidence suggests that the non-structural protein 4 from Virus X can influence viral tropism, leading to the localization of the virus in the swim bladder of zebrafish during infection. These results challenge the current understanding that viral tropism is governed solely by viral structural interactions with host receptors. This indicates a potentially novel mechanism of host-pathogen interactions that requires further exploration. Moreover, this study highlights the versatility of zebrafish as a powerful *in vivo* model for studying viral infections. Their optical transparency enables real-time visualization of viral replication and infection. Their suitability for infectivity assays and antiviral drug testing allows researchers to track viral tropism *in vivo* within a model that closely reflects a clinically relevant living organism. However, the first step for future work based on the results presented in this report would be to repeat the HRM analysis using optimized primers to validate the genotypes of crispant zebrafish, thereby providing more complete and compelling evidence.

While this study was not able to identify specific therapeutic targets for alphavirus infection, these insights opened up a new pathway to further understand host-pathogen interactions. A deeper analysis of the interaction between MXRA8 and X WT, as well as IRF3 and CHIKV WT, is needed. It is important to identify the domains or downstream processes that lead to the interactions observed in this study and to determine if the same effect occurs when only those domains or processes are depleted. This is crucial for identifying a therapeutic target for alphaviruses. Since MXRA8 and IRF3 have crucial functions in the host, it is not feasible to use the whole protein as a target, as it will disrupt normal host function, which was seen in this study, where knocking out IRF3 led to over 50% mortality rate of the zebrafish embryos.

Additionally, to better understand which receptors are binding to the virus, a genetically engineered virus with an epitope tag, such as a His-tag, can be cloned. The zebrafish would then be infected with the tagged virus before extracting all the proteins from the zebrafish. The extracted protein could then be subjected to affinity chromatography to obtain a pure sample of the tagged virus and the host receptor bound to it. The receptor can then be identified via Mass Spectrometry to identify host receptors and factors involved in virus entry and host-virus interactions. Other receptors that have been previously identified to be involved in alphavirus entry in an *in vitro* setting should also be evaluated using the *in vivo* zebrafish animal model.

To further understand the viral tropism that seems to be caused by a viral nsP, a larger sample size should be used to obtain sufficient data points for accurate statistical analysis. The receptors and host factors found in the tissue surrounding the swim bladder also need to be further understood. If the host factors can be understood, then a deeper analysis to identify which domain of the nsP is responsible for this tropism could be conducted, permitting a better understanding of the alphavirus genome and its functions. With a better understanding of the virus-host interactions, novel therapeutic designs can be developed.

## 6. References

1. *An Interactive atlas of Zebrafish Vascular Anatomy* (2025).  
<https://zfish.nichd.nih.gov/FinalDesign1/frame1b%283d%29.html> [Accessed 8 July 2025].
2. Azar, S.R. *et al.* (2020) 'Epidemic alphaviruses: Ecology, emergence and outbreaks,' *Microorganisms*, 8(8), p. 1167. <https://doi.org/10.3390/microorganisms8081167>.
3. Basore, K. *et al.* (2019) "Cryo-EM Structure of Chikungunya Virus in Complex with the Mxra8 Receptor," *Cell*, 177(7), pp. 1725-1737.e16.  
<https://doi.org/10.1016/j.cell.2019.04.006>.
4. Beck, A.P., Watt, R.M. and Bonner, J. (2014) "Dissection and lateral mounting of zebrafish embryos: Analysis of spinal cord development," *Journal of Visualized Experiments* [Preprint], (84). <https://doi.org/10.3791/50703>.
5. Bernard, E. *et al.* (2010) "Endocytosis of Chikungunya Virus into Mammalian Cells: Role of Clathrin and Early Endosomal Compartments," *PLoS ONE*, 5(7), p. e11479.  
<https://doi.org/10.1371/journal.pone.0011479>.
6. Chee, F.Y. *et al.* (2016) "Epidemiological risk factors for adult dengue in Singapore: an 8-year nested test negative case control study," *BMC Infectious Diseases*, 16(1).  
<https://doi.org/10.1186/s12879-016-1662-4>.
7. *Chikungunya virus disease worldwide overview* (2025).  
<https://www.ecdc.europa.eu/en/chikungunya-monthly> [Accessed 11 July 2025].

8. Choi, T.-Y. *et al.* (2021) “Zebrafish as an animal model for biomedical research,” *Experimental & Molecular Medicine*, 53(3), pp. 310–317.  
<https://doi.org/10.1038/s12276-021-00571-5>.
9. *Communicable Diseases Surveillance in Singapore 2013* (no date).  
<https://www.cda.gov.sg/resources/communicable-diseases-surveillance-in-singapore-2013> [Accessed 10 July 2025].
10. Crouzier, L. *et al.* (2021) “Use of zebrafish models to boost research in rare genetic diseases,” *International Journal of Molecular Sciences*, 22(24), p. 13356.  
<https://doi.org/10.3390/ijms222413356>.
11. De Caluwé, L. *et al.* (2021) “The CD147 protein complex is involved in entry of chikungunya virus and related alphaviruses in human cells,” *Frontiers in Microbiology*, 12. <https://doi.org/10.3389/fmicb.2021.615165>.
12. De Lima Cavalcanti, T.Y.V. *et al.* (2022) “A review on chikungunya virus epidemiology, pathogenesis and current vaccine development,” *Viruses*, 14(5), p. 969. <https://doi.org/10.3390/v14050969>.
13. Debaenst, S. *et al.* (2024) “Crispant analysis in zebrafish as a tool for rapid functional screening of disease-causing genes for bone fragility,” *eLife*, 13.  
<https://doi.org/10.7554/elife.100060>.
14. Desdouits, M. *et al.* (2015) “Genetic characterization of Chikungunya virus in the Central African Republic,” *Infection Genetics and Evolution*, 33, pp. 25–31.  
<https://doi.org/10.1016/j.meegid.2015.04.006>.

15. Díaz-Pascual, F. et al. (2017) "In vivo Host-Pathogen Interaction as Revealed by Global Proteomic Profiling of Zebrafish Larvae," *Frontiers in Cellular and Infection Microbiology*, 7. <https://doi.org/10.3389/fcimb.2017.00334>.
16. Fongsaran, C. et al. (2014) "Involvement of ATP synthase β subunit in chikungunya virus entry into insect cells," *Archives of Virology*, 159(12), pp. 3353–3364. <https://doi.org/10.1007/s00705-014-2210-4>.
17. Franzia, M. et al. (2024) "Zebrafish (*Danio rerio*) as a Model System to Investigate the Role of the Innate Immune Response in Human Infectious Diseases," *International Journal of Molecular Sciences*, 25(22), p. 12008. <https://doi.org/10.3390/ijms252212008>.
18. Freitas, A.R.R. et al. (2024) "Excess mortality associated with chikungunya epidemic in Southeast Brazil, 2023," *Frontiers in Tropical Diseases*, 5. <https://doi.org/10.3389/fitd.2024.1466207>.
19. Frumence, E. et al. (2025) "Genomic insights into the re-emergence of chikungunya virus on Réunion Island, France, 2024 to 2025," *Eurosurveillance*, 30(22). <https://doi.org/10.2807/1560-7917.es.2025.30.22.2500344>.
20. Hapuarachchi, H.C. et al. (2021) 'Transient transmission of Chikungunya virus in Singapore exemplifies successful mitigation of severe epidemics in a vulnerable population,' *International Journal of Infectious Diseases*, 110, pp. 417–425. <https://doi.org/10.1016/j.ijid.2021.08.007>.
21. Hiscox, A. et al. (2025) "An exploration of current and future vector-borne disease threats and opportunities for change," *Frontiers in Public Health*, 13. <https://doi.org/10.3389/fpubh.2025.1585412>.

22. Holmes, A.C. *et al.* (2020) “A molecular understanding of alphavirus entry,” *PLoS Pathogens*, 16(10), p. e1008876. <https://doi.org/10.1371/journal.ppat.1008876>.
23. Hoornweg, T.E. *et al.* (2016) “Dynamics of chikungunya virus cell entry unraveled by Single-Virus tracking in living cells,” *Journal of Virology*, 90(9), pp. 4745–4756. <https://doi.org/10.1128/JVI.03184-15>.
24. Hoshijima, K. *et al.* (2019) “Highly Efficient CRISPR-Cas9-Based Methods for Generating Deletion Mutations and F0 Embryos that Lack Gene Function in Zebrafish,” *Developmental Cell*, 51(5), pp. 645-657.e4. <https://doi.org/10.1016/j.devcel.2019.10.004>.
25. *Immunofluorescence protocol for frozen sections* (no date). <https://sites.wustl.edu/cavallilab/items/immunofluorescence-protocol-for-frozen-sections/> [Accessed 9 July 2025].
26. Jupp, P.G., PhD *et al.* (2008) “RISK FACTORS FOR TRANSMISSION OF CHIKUNGUNYA VIRUS INFECTION IN SINGAPORE, 2008,” *Journal of Epidemiology and Community Health*, 62, pp. xi–xiii. <https://isomer-user-content.by.gov.sg/3/8f43ff66-22a5-4d77-98ca-6a40be822d51/special-feature-malaria-and-norovirus-2008.pdf> [Accessed 8 July 2025].
27. Keeley, S. *et al.* (2025) “Rapid and robust generation of cardiomyocyte-specific crisprants in zebrafish using the cardiodeleter system,” *Cell Reports Methods*, 5(3), p. 101003. <https://doi.org/10.1016/j.crmeth.2025.101003>.
28. Kim, D.Y. *et al.* (2016) “New world and Old world alphaviruses have evolved to exploit different components of stress granules, FXR and G3BP proteins, for

- assembly of viral replication complexes," *PLoS Pathogens*, 12(8), p. e1005810. <https://doi.org/10.1371/journal.ppat.1005810>.
29. Lantz, A.M. and Baxter, V.K. (2025) "Neuropathogenesis of old world alphaviruses: Considerations for the development of medical countermeasures," *Viruses*, 17(2), p. 261. <https://doi.org/10.3390/v17020261>.
30. Lello, L.S. *et al.* (2021) 'NSP4 is a major determinant of alphavirus replicase activity and template selectivity,' *Journal of Virology*, 95(20). <https://doi.org/10.1128/jvi.00355-21>.
31. Li, Y. *et al.* (2021) "The importance of glycans of viral and host proteins in enveloped virus infection," *Frontiers in Immunology*, 12. <https://doi.org/10.3389/fimmu.2021.638573>.
32. Liyanage, S. *et al.* (2017) "Optimization and validation of cryostat temperature conditions for trans-reflectance mode FTIR microspectroscopic imaging of biological tissues," *MethodsX*, 4, pp. 118–127. <https://doi.org/10.1016/j.mex.2017.01.006>.
33. Ma, H. *et al.* (2020) "LDLRAD3 is a receptor for Venezuelan equine encephalitis virus," *Nature*, 588(7837), pp. 308–314. <https://doi.org/10.1038/s41586-020-2915-3>.
34. Maginnis, M.S. (2018) "Virus–Receptor interactions: the key to cellular invasion," *Journal of Molecular Biology*, 430(17), pp. 2590–2611. <https://doi.org/10.1016/j.jmb.2018.06.024>.
35. Mengstie, M.A. and Wondimu, B.Z. (2021) "Mechanism and applications of CRISPR/CAS-9-Mediated Genome Editing," *Biologics*, Volume 15, pp. 353–361. <https://doi.org/10.2147/btt.s326422>.

36. Ng, L.-C. *et al.* (2009) "Entomologic and Virologic Investigation of Chikungunya, Singapore," *Emerging Infectious Diseases*, 15(8), pp. 1243–1249.  
<https://doi.org/10.3201/eid1508.081486>.
37. Paredes, A. *et al.* (2006) "Structural biology of old world and new world alphaviruses," *Springer eBooks*, pp. 179–185. [https://doi.org/10.1007/3-211-29981-5\\_14](https://doi.org/10.1007/3-211-29981-5_14).
38. Parvez, S., Brandt, Z.J. and Peterson, R.T. (2023) "Large-scale F0 CRISPR screens in vivo using MIC-Drop," *Nature Protocols*, 18(6), pp. 1841–1865.  
<https://doi.org/10.1038/s41596-023-00821-y>.
39. Quetglas, J.I. *et al.* (2010) "Alphavirus vectors for cancer therapy," *Virus Research*, 153(2), pp. 179–196. <https://doi.org/10.1016/j.virusres.2010.07.027>.
40. Rogers, K.J. *et al.* (2020) 'TF protein of Sindbis virus antagonizes host type I interferon responses in a palmitoylation-dependent manner,' *Virology*, 542, pp. 63–70. <https://doi.org/10.1016/j.virol.2020.01.001>.
41. Rudd, P.A. *et al.* (2012) "Interferon Response Factors 3 and 7 Protect against Chikungunya Virus Hemorrhagic Fever and Shock," *Journal of Virology*, 86(18), pp. 9888–9898. <https://doi.org/10.1128/jvi.00956-12>.
42. Sant, K.E. and Timme-Laragy, A.R. (2018) "Zebrafish as a model for toxicological perturbation of yolk and nutrition in the early embryo," *Current Environmental Health Reports*, 5(1), pp. 125–133. <https://doi.org/10.1007/s40572-018-0183-2>.
43. Santos, L.G. *et al.* (2024) "Chikungunya chronic arthralgia: impact on general and mental health and absenteeism from work," *Revista Da Sociedade Brasileira De Medicina Tropical*, 57. <https://doi.org/10.1590/0037-8682-0149-2024>.

44. Schuffenecker, I. *et al.* (2006) “Genome microevolution of chikungunya viruses causing the Indian Ocean outbreak,” *PLoS Medicine*, 3(7), p. e263.  
<https://doi.org/10.1371/journal.pmed.0030263>.
45. See, N.L.C. and S. (2013) “Govt budget for dengue prevention rises to S\$85m in 2013,” *TODAY*, 18 July. <https://www.todayonline.com/singapore/govt-budget-dengue-prevention-rises-s85m-2013> [Accessed 8 July 2025].
46. Shin, G. *et al.* (2012) “Structural and functional insights into alphavirus polyprotein processing and pathogenesis,” *Proceedings of the National Academy of Sciences*, 109(41), pp. 16534–16539. <https://doi.org/10.1073/pnas.1210418109>.
47. Silva, L.A. and Dermody, T.S. (2017) “Chikungunya virus: epidemiology, replication, disease mechanisms, and prospective intervention strategies,” *Journal of Clinical Investigation*, 127(3), pp. 737–749. <https://doi.org/10.1172/jci84417>.
48. Słomka, M. *et al.* (2017) “High Resolution Melting (HRM) for High-Throughput Genotyping—Limitations and caveats in Practical case studies,” *International Journal of Molecular Sciences*, 18(11), p. 2316.  
<https://doi.org/10.3390/ijms18112316>.
49. Sofyantoro, F. *et al.* (2024) “Zebrafish as a model organism for virus disease research: Current status and future directions,” *Heliyon*, 10(13), p. e33865.  
<https://doi.org/10.1016/j.heliyon.2024.e33865>.
50. Solignat, M. *et al.* (2009) “Replication cycle of chikungunya: A re-emerging arbovirus,” *Virology*, 393(2), pp. 183–197. <https://doi.org/10.1016/j.virol.2009.07.024>.

51. Song, H. et al. (2019) "Molecular basis of arthritogenic alphavirus receptor MXRA8 binding to chikungunya virus envelope protein," *Cell*, 177(7), pp. 1714-1724.e12.  
<https://doi.org/10.1016/j.cell.2019.04.008>.
52. Suhrbier, A., Jaffar-Bandjee, M.-C. and Gasque, P. (2012) 'Arthritogenic alphaviruses—an overview,' *Nature Reviews Rheumatology*, 8(7), pp. 420–429.  
<https://doi.org/10.1038/nrrheum.2012.64>.
53. Thuaud, F. et al. (2013) "Prohibitin Ligands in Cell Death and Survival: Mode of action and therapeutic potential," *Chemistry & Biology*, 20(3), pp. 316–331.  
<https://doi.org/10.1016/j.chembiol.2013.02.006>.
54. Tong, S., Jun, K.T.Y. and Carissimo, G. (2024) "Pathogenicity and virulence of O'nyong-nyong virus: A less studied Togaviridae with pandemic potential," *Virulence*, 15(1). <https://doi.org/10.1080/21505594.2024.2355201>.
55. Treffers, E.E. et al. (2023) "The alphavirus nonstructural protein 2 NTPase induces a host translational shut-off through phosphorylation of eEF2 via cAMP-PKA-eEF2K signaling," *PLoS Pathogens*, 19(2), p. e1011179.  
<https://doi.org/10.1371/journal.ppat.1011179>.
56. Uchime, O., Fields, W. and Kielian, M. (2013) "The Role of E3 in pH Protection during Alphavirus Assembly and Exit," *Journal of Virology*, 87(18), pp. 10255–10262.  
<https://doi.org/10.1128/jvi.01507-13>.
57. Wang, S., Mahalingam, S. and Merits, A. (2025) "Alphavirus NSP2: a multifunctional regulator of viral replication and promising target for Anti-Alphavirus therapies," *Reviews in Medical Virology*, 35(2). <https://doi.org/10.1002/rmv.70030>.

58. Weaver, S.C. et al. (2012) “Chikungunya virus and prospects for a vaccine,” *Expert Review of Vaccines*, 11(9), pp. 1087–1101. <https://doi.org/10.1586/erv.12.84>.
59. *What is High Resolution Melting (HRM)?* (2025). <https://www.bio-rad.com/en-sg/applications-technologies/what-high-resolution-melting-hrm?ID=LUSOIH97Q> [Accessed 10 July 2025].
60. White, L.K. et al. (2010) “Chikungunya virus induces IPS-1-Dependent innate immune activation and protein kinase R-Independent translational shutoff,” *Journal of Virology*, 85(1), pp. 606–620. <https://doi.org/10.1128/jvi.00767-10>.
61. Wintachai, P. et al. (2012) “Identification of prohibitin as a Chikungunya virus receptor protein,” *Journal of Medical Virology*, 84(11), pp. 1757–1770. <https://doi.org/10.1002/jmv.23403>.
62. Yanai, H. et al. (2018) “Revisiting the role of IRF3 in inflammation and immunity by conditional and specifically targeted gene ablation in mice,” *Proceedings of the National Academy of Sciences*, 115(20), pp. 5253–5258. <https://doi.org/10.1073/pnas.1803936115>.
63. Zhang, R. et al. (2018) “Mxra8 is a receptor for multiple arthritogenic alphaviruses,” *Nature*, 557(7706), pp. 570–574. <https://doi.org/10.1038/s41586-018-0121-3>.
64. Zimmerman, O. et al. (2023) “Entry receptors — the gateway to alphavirus infection,” *Journal of Clinical Investigation*, 133(2). <https://doi.org/10.1172/jci165307>.